frontiers | Frontiers in Earth Science

TYPE Review
PUBLISHED 08 August 2022
DOI 10.3389/feart.2022.904787

OPEN ACCESS

EDITED BY
John L. Isbell,
University of Wisconsin–Milwaukee, United States

REVIEWED BY
Christopher Fielding,
University of Connecticut, United States
György Varga,
Research Centre for Astronomy and Earth Sciences, Hungary

*CORRESPONDENCE
Gerilyn S. Soreghan,
Lsoreg@ou.edu

SPECIALTY SECTION
This article was submitted to Sedimentology, Stratigraphy and Diagenesis, a section of the journal Frontiers in Earth Science

RECEIVED 25 March 2022
ACCEPTED 30 June 2022
PUBLISHED 08 August 2022

CITATION
Soreghan GS, Pfeifer LS, Sweet DE and Heavens NG (2022), Detecting upland glaciation in Earth's pre-Pleistocene record.
Front. Earth Sci. 10:904787.
doi: 10.3389/feart.2022.904787

Detecting upland glaciation in Earth's pre-Pleistocene record

Gerilyn S. Soreghan[1]*, Lily S. Pfeifer[1], Dustin E. Sweet[2] and Nicholas G. Heavens[3]

[1]School of Geosciences, University of Oklahoma, Norman, OK, United States, [2]Department of Geosciences, Texas Tech University, Lubbock, TX, United States, [3]Space Science Institute, Boulder, CO, United States

Earth has sustained continental glaciation several times in its past. Because continental glaciers ground to low elevations, sedimentary records of ice contact can be preserved from regions that were below base level, or subject to subsidence. In such regions, glaciated pavements, ice-contact deposits such as glacial till with striated clasts, and glaciolacustrine or glaciomarine strata with dropstones reveal clear signs of former glaciation. But assessing upland (mountain) glaciation poses particular challenges because elevated regions typically erode, and thus have extraordinarily poor preservation potential. Here we propose approaches for detecting the former presence of glaciation in the absence or near-absence of ice-contact indicators; we apply this specifically to the problem of detecting upland glaciation, and consider the implications for Earth's climate system. Where even piedmont regions are eroded, pro- and periglacial phenomena will constitute the primary record of upland glaciation. Striations on large (pebble and larger) clasts survive only a few km of fluvial transport, but microtextures developed on quartz sand survive longer distances of transport, and record high-stress fractures consistent with glaciation. Proglacial fluvial systems can be difficult to distinguish from non-glacial systems, but a preponderance of facies signaling abundant water and sediment, such as hyperconcentrated flood flows, non-cohesive fine-grained debris flows, and/or large-scale and coarse-grained cross-stratification are consistent with proglacial conditions, especially in combination with evidence for cold temperatures, such as rip-up clasts composed of noncohesive sediment, indicating frozen conditions, and/or evidence for a predominance of physical over chemical weathering. Other indicators of freezing (periglacial) conditions include frozen-ground phenomena such as fossil ice wedges and ice crystals. Voluminous loess deposits and eolian-marine silt/mudstone characterized by silt modes, a significant proportion of primary silicate minerals, and a provenance from non-silt precursors can indicate the operation of glacial grinding, even though such deposits may be far removed from the site(s) of glaciation. Ultimately, in the absence of unambiguous ice-contact indicators, inferences of glaciation must be grounded on an array of observations that together record abundant meltwater, temperatures capable of sustaining glaciation, and glacial weathering (e.g., glacial grinding). If such arguments are viable, they can bolster the accuracy of past climate models, and guide climate modelers in assessing the types of forcings that could enable glaciation at elevation, as well as the

extent to which (extensive) upland glaciation might have influenced global climate.

KEYWORDS

mountain glaciation, alpine glaciation, proglacial, periglacial, ice-contact, loess, cold-weathering, microtextures

1 Introduction

Detection of glaciation in Earth's past relies on erosional landforms and—especially for Earth's deep-time record—the ice-contact sediments left behind. Wegener (1929) asserted that "Generally, it is usual to regard the rock as certainly glacial only if one has been able still to detect the polished surface of the outcrop under the boulder clay of the ground moraine." This approach works reasonably well for the near-time (Quaternary) record, and—in the case of ice sheets that ground below base level—the sedimentary record of ice contact can be preserved in deep time. In this case, the attributes that meet Wegener's (1929) high standard, such as striated, polished, and/or grooved bedrock surfaces, diamictites with striated clasts, glacio-tectonized strata, and dropstones enable geoscientists to detect "icehouse" climates characterized by continental glaciation dating from intervals millions and even billions of years in Earth's past (e.g., Crowell, 1978; Crowell, 1999; Benn and Evans, 2010).

But preservational bias pervades the deep-time record, wherein most sedimentary strata record conditions in regions near or below base-level within tectonically subsiding regions; in contrast to such settings, upland or "mountain" glaciation in particular occurs in regions characterized by erosion rather than deposition. Upland glaciation should have been common during Earth's icehouse states and may have occurred even in presumed greenhouse intervals. However, without the preservation of mountainous terrain—a tall order for Earth's deep-time record—the only sign of glaciation might be ice-proximal strata from the proglacial region, or even periglacial regions relatively far removed from the ice margin.

Although geoscientists can study sediments derived from uplands to understand the tectonics of the uplands (e.g., Reiners and Brandon, 2006), the climatic attributes are largely lost, since sediments primarily record environmental conditions of their sites of deposition—in subsiding basins. Yet, establishing the former presence of glaciation in uplands is key for studies of past climates given the extreme sensitivity of mountain glaciation to climate change (e.g., Kaser, 2009; Russell et al., 2009), and the importance of mountain glaciers as potential climate drivers. The differentiation of upland (mountain) glaciation from continental glaciation hinges to some degree on evidence for the (former) presence of a discrete paleouplift (e.g., zero-isopach area). Where erosion has completely removed the upland stratigraphic and geomorphic record, however, we posit that upland glaciation can be inferred on the basis of an association of evidence (facies and attributes) that indicates pro- and/or periglacial conditions proximal to the inferred paleoupland. In this contribution, we outline attributes to potentially recognize these conditions. Such inferences will remain interpretative and equivocal, but we argue that a preponderance of observations consistent with a glacial influence yet lacking ice-contact facies or surfaces should not necessarily preclude an interpretation of upland glaciation. Of course, where uplands remain, the ultimate test is discovery of preserved glacial landforms (e.g., paleovalleys) and ice-contact deposits on the upland itself.

2 Definition of upland (mountain) glaciation

In the modern and recent record, "mountain" (also termed "alpine") glaciation refers to glaciation in or confined by mountainous terrain, in contrast to ice sheets that are unconstrained by topography (Benn and Evans, 2010). However, this definition—like many features of glacial systems—relies heavily on geomorphology, reflecting the bias of our modern life on an icehouse Earth. In deep (pre-Cenozoic) time, we lose many of the landform features, leaving primarily the sedimentary deposits. Moreover, evidence for glaciation in Earth's deep-time record is biased towards evidence for continental glaciation since mountains tend to erode. Despite these preservational challenges, mountain glaciation has been asserted for some deep-time periods where glaciation terminated into subsiding regions, notably from the late Paleozoic of South America and Australia. For example, Lopez-Gamundi et al. (1994) inferred mountain glaciation for the Argentinian preCordillera on the basis of (glacial) paleocurrent vectors that radiated from basement highs. Other interpretations of mountain glaciation are similarly based on data indicating the (inferred) locations of late Paleozoic highlands (e.g., Australia and the Argentina proto-Precordillera; Crowell, 1999; Henry et al., 2010). Jones and Fielding (2008) hypothesized mountain glaciation in the late Paleozoic record of Australia on the basis of significant amounts of debris and abrupt lateral changes in thickness and character of stratal successions, although these criteria are somewhat vague. Several authors (Lopez-Gamundi et al., 1994; Kneller et al., 2004; Dykstra et al., 2006; Limarino et al., 2006; Aquino et al., 2014; Moxness et al., 2018; Valdez-Buso et al., 2020; Lopez-Gamundi et al., 2021) have identified glacial paleovalleys cut into the Argentinian proto-Precordillera, although the existence of a paleovalley alone does not confer evidence for mountain glaciation, since valley glaciers today—e.g., Greenland—occur where outlet glaciers drain ice sheets through regions with some topographic relief. Isbell et al. (2003) and Isbell et al. (2012) suggested that the volume of glacial

TABLE 1 Attributes of pro- and periglacial settings illustrated in this paper.

Quartz grain microtextures	• Deep troughs (>10 μm-deep)	Figure 1A
	• Straight/linear grooves (<10 μm-deep)	Figures 1B,D
	• Conchoidal fractures	Figure 1C
Fluvial facies	• Scour-and-fill deposits (10–50 cm)	Figure 3A
	• Mega crossbeds (up to 2.5 m)	Figures 3D,E
	• Floating clasts, HFF deposits (~10–30 cm diam.)	Figures 3B,C,L
	• Pebbly mud flows and rip up clasts	Figures 3J,K,H–I
	• Sandstone dykes (mm-cm-scale)	Figure 3K
Frozen ground phenomena	• Polygonal cracking (20–75 cm)	Figures 5A,B
	• Frost wedging (up to meter-scale)	Figure 5C
	• Ice crystal pseudomorphs (2–3 cm diameter)	Figures 5D–F
Loess and eolian-transported dust	• Massive (structureless) bedding (up to 20 m)	Figures 6A,B
	• Blocky-to-angular fracturing	Figures 6C,D
	• Slickensides, pedogenic (5–10 cm)	Figure 6E
	• Root traces (0.5–1 m)	Figure 6F
	• Predominance of siliciclastic silt	Figure 7

deposits, the nature of the facies, and variable, or radial paleocurrent vectors confer means to differentiate between ice sheets and mountain glaciers, but the details remain murky. Despite the challenge of deep-time preservation of upland systems, we postulate that mountain glaciation can be interpreted using multiple lines of evidence from sedimentary facies and attributes that potentially record 1) proximity to glaciated paleohighlands, and 2) operation of processes either unique to, or common in glacial systems.

3 Indicators of glaciation outside the zone of ice contact

In the absence of ice-contact deposits, we must rely upon secondary deposits and features (Table 1) in pro- and periglacial regions that carry traces of glacial processes, and/or of cold-climate conditions. Although definitions vary somewhat, we take proglacial processes to be those that occur in proximity to the ice margin, whereas periglacial processes imply cold, non-glacial environments (Benn and Evans, 2010; French, 2013).

3.1 Quartz-grain microtextures

Glaciers abrade rock surfaces by striating and polishing them, and striae on bedrock or clasts have long been the gold standard for recognition of glaciation, provided they can be distinguished confidently from other striae-producing processes e.g., mass movements and tectonics (Hambrey, 1994; Atkins, 2003). But striae are both lithology dependent and readily erased: they develop preferentially on fine-grained and soft lithologies (rarely on granite or gneiss; Anderson, 1955; Boulton, 1979; Kuhn et al., 1993; Benn and Evans, 2010), and typically survive only 1–2 km of fluvial transport (Atkins, 2003). Furthermore, they are relatively rare: in systematic grid analyses of glacial systems, <10%–20% of clasts exhibited striae (Anderson, 1955; Atkins, 2004). Facets on clasts can survive transport of up to 5–6 km (Atkins, 2003)—still a relatively short distance.

In contrast, microtextures on individual grains of minerals, most commonly quartz, have been posited as a means to infer glacial processes (e.g., Krinsley and Doornkamp, 1973; Mahaney, 2002), and they preserve far longer in fluvial transport (e.g., Sweet and Brannan, 2016). Assessment of specific conditions that resulted in the microtextures preserved on quartz grains can be challenging since many individual microtextures can be produced under different transport conditions and environments (Brown, 1973). More recent work has argued that only large-scale fractures that cover at least one-quarter of the grain surface can be considered glaciogenic, as smaller-scale fractures can be produced in a wide variety of environments (Molen, 2014). Despite these limitations, a growing body of work suggests that suites of microtextures, rather than a single diagnostic feature, can be used to differentiate among transport media. For example, grains that have undergone saltation or bed load transport in modern systems and experiments commonly exhibit v-shaped cracks as well as edge rounding (Sweet and Brannan, 2016; Costa et al., 2017;

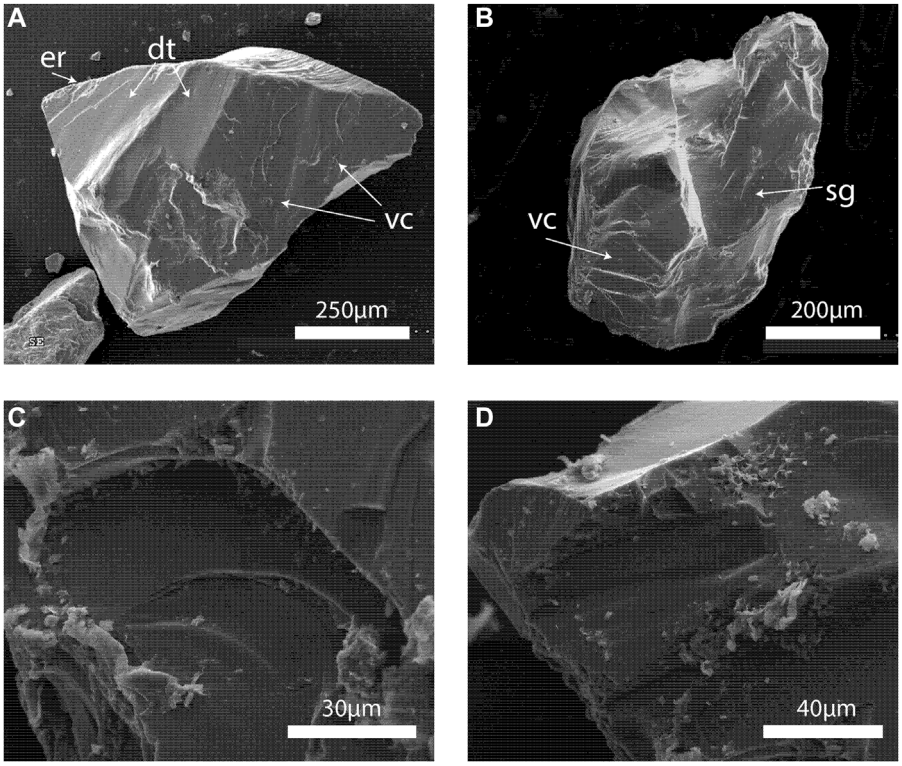

FIGURE 1
SEM micrographs demonstrating the character and preservation of glacial influence on grain transport. **(A,B)** grains collected in modern fluvial system, 65 km down the Chitina River from the terminal moraine of the Chitina Glacier (AK, United States; see Sweet and Brannan, 2016). **(A)** Undulose surface on quartz grain with grooves >10 μm deep, termed deep troughs (dt). Grain has experienced percussion overprinting due to saltation during fluvial transport as indicated by edge rounding (er) and v-shaped cracks (vc). **(B)** Linear groove <10 μm deep on the fracture surface, termed straight grooves (sg). Percussion influence on grain is demonstrated by abundant chipping at grain edges that manifest as arcuate steps and conchoidal fractures as well as numerous v-shaped cracks (vc). Note only one v-shaped crack is identified in the micrograph, but numerous occurrences are present. **(C,D)** grains collected in Permo-Pennsylvanian Cutler Formation (interpreted proglacial fluvial system; see Keiser et al., 2015) showing microtextures including conchoidal fractures **(C)** and linear grooves (<10 μm deep). See Sweet and Soreghan (2010b) for classifications of transport-induced microtextures on quartz grain surfaces.

Smith et al., 2018). Glacial till from upland glaciers may harbor a suite of microstriae on grains (Hart, 2006; Sweet and Brannan, 2016; Kalinska et al., 2021). Ice sheets can produce microtextures that differ from those imparted by upland glaciation owing to the different thicknesses of ice in these systems (Mahaney et al., 1988; Mahaney and Kalm, 1995), although we focus here specifically on upland glacial systems.

Sweet and Soreghan (2010a) proposed a tripatite nomenclature to differentiate microtextures imparted by different types of stresses: percussion fractures, high-stress fractures, and polygenetic fractures. Percussion microtextures consist of v-shaped cracks and edge rounding, and are common to eolian, coastal, and fluvial systems. High-stress microtextures consist of grooves, troughs, and gouges (Figure 1) resulting from grain-to-grain contact under sustained shear stress and are common in grains recovered from till and proglacial deposits (Mahaney and Kalm, 1996; Hart, 2006; Sweet and Brannan, 2016; Smith et al., 2018; Kalinska et al., 2021; Reahl et al., 2021), but also are reported from structural shear zones and debris flows (Mahaney, 2002). Polygenetic microtextures are the remainder of the mechanically induced microtextures observable on grain surfaces and originate through various processes. Since the development of this tripartite suite of microtextures, numerous studies from ancient environments have employed this approach to differentiate between glacial and sub-aqueous or sub-aerial percussion transport (Kirshner and Anderson, 2011; Witus et al., 2014; Keiser et al., 2015; Kalinska-Nartisa et al., 2017; Nartiss and Kalinska-Nartisa, 2017; Kalinska-Nartisa et al., 2018; Kalinska-Nartisa and Galka, 2018). Statistical tests of the tripartite system from modern settings demonstrate that percussion textures prevail in fluvial environments (Smith et al., 2018; Reahl et al., 2021), but Reahl et al. (2021) suggested that high-stress microtextures carry more ambiguity, as some eolian systems exhibit a higher incidence of high-stress features than glacial systems; for example, upturned plates are a microtexture

TABLE 2 Dimensions of glaciers and slopes of proglacial systems studied in Sweet and Brannan (2016), Pippin (2016), and Kalinska et al. (2021).

Glacier	Length (km)	Avg. width (km)	Icefield area (km^2)	Avg. slope	Avg. proglacial slope
Virkisjökull	4.8	0.8	10	0.175	0.034
Salmon	15.7	1.5	82	0.064	0.017
Chitina tongue 1	54	2.3		0.03	
Chitina tongue 2	82.5	3	4,856	0.025	0.006
Chitina tongue 3	82.7	4.4		0.022	

common to both eolian and glacial deposits (c.f. Mahaney and Kalm, 1995; Li et al., 2020a). However, all of those high-stress microtexture occurrences are from eolian systems located in proximity to a glacial influence, obfuscating whether the features were created during glacial or eolian transport. The probability of high-stress microtextures occurring that reflect microstriae, such as grooves and troughs, is extremely low in eolian systems far removed from modern or Pleistocene glaciation (Reahl et al., 2021). Moreover, samples collected in fluvial systems far removed from a glacial influence yielded very low probabilities of retaining a high-stress signal (Reahl et al., 2021). Thus, while high-stress microtextures have been reported from deposits other than those of glacial origin, most of the reported occurrences are associated with glaciation. Multiple studies show that high-stress microtextures are progressively overprinted downstream from a glacial terminus (Pippin, 2016; Sweet and Brannan, 2016; Krizek et al., 2017; Smith et al., 2018; Kalinska et al., 2021). In a glaciofluvial system, the ratio between percussion and high-stress microtextures observed on quartz grains decreases downstream from the glacier with ~10% of the grains still exhibiting high-stress microtextures within ~200 km of the glacial terminus (Sweet and Brannan, 2016) and the preservation of microstriae indicates a period of glacial influence during the transport history of these grains.

While we posit that high-stress microtextures can indicate a past glacial influence, the total number of quartz grains that exhibit high-stress microtextures varies by study. Near the glacial terminus, fractions of grains exhibiting high-stress values range from ~10% to 30%, whereas polygenetic microtextures are reported on 60%–80% of the grains examined (Sweet and Brannan, 2016; Kalinska et al., 2021). Moreover, Reahl et al. (2021) reported that the largest individual source of variance in the data is operator bias. This variance might be resolvable given more studies of modern systems using a double-blind approach and quantitative data analyses, such as used in Smith et al. (2018). Alternatively, variations in ice volume and thus total energy imparted onto grains might also cause such variation. For example, the area, width, and length of the glaciers and slopes of the proglacial systems used in the Sweet and Brannan (2016) and Kalinska et al. (2021) studies vary significantly (Table 2). While ice thickness has been cited as a control on the type and abundance of microtextures observed in ice-sheet versus upland glacial deposits (Mahaney et al., 1988; Mahaney, 1995; Mahaney et al., 1996), no systematic study exists to assess quartz-grain microtextural variation due to thickness of ice in alpine settings.

3.1.1 Case study: Quartz grain microtextures in the Pennsylvanian-lower Permian Cutler Formation (Colorado, United States)

The Cutler Formation that crops out near Gateway, Colorado (United States; Figure 2) has been hypothesized to record proglacial deposition based on the presence of an inferred late Paleozoic glacially carved valley within the uplands (Soreghan et al., 2007; Soreghan et al., 2008a; Patterson et al., 2021), inferred ice-contact facies in the most proximal deposits onlapping the paleo-upland (Soreghan et al., 2008b; Soreghan et al., 2009), microstriae on quartz grains (Keiser et al., 2015), and inferred proglacial fluvial deposition (see discussion in 3.2.5. Case study below; Soreghan et al., 2009; Sweet, 2017). Note that the Cutler Formation extends from the ancient Uncompahgre highland to the distal Paradox basin that bordered the highland, but we focus here on the proximal-most Cutler system, exposed within <1–10 km of the paleohighland. In this system, quartz grain microtextures demonstrate a facies-dependent variability in the percentage of grains exhibiting percussion features, but a sustained 10%–15% of the grains exhibit high-stress microtextures (e.g., Figures 1C,D; Keiser et al., 2015). This indicates that: 1) the type of deposit sampled for microtextural analysis is less important in this system when the goal is identifying a glacial influence on grain transport, and 2) grains likely acquired the high-stress microtextures prior to entering the fluvial system of the Cutler Formation. Regionally, within coeval strata of central Colorado, Sweet and Soreghan (2010a) reported high-stress microtextures in the uplift-proximal alluvial setting of the Fountain Formation exposed within <50 km of the Ute Pass paleohighland, which they called upon to posit upland glaciation in this paleohighland as well.

3.2 Facies common to proglacial fluvial systems

Proglacial systems are characterized by an abundance of both water and sediment (Maizels, 1997). Similar to other fluvial and

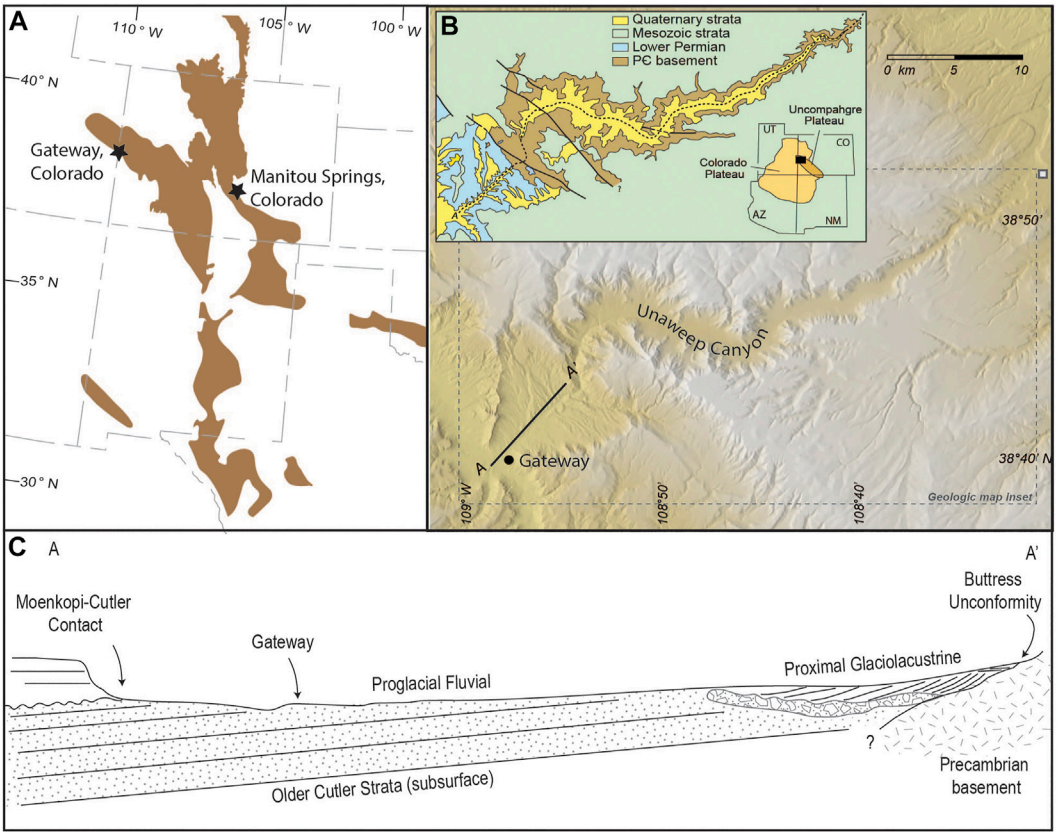

FIGURE 2
Location map and depositional architecture of the proximal Cutler Formation. **(A)** Upland areas during the late Paleozoic (brown polygons). Proximal Cutler and Fountain formations discussed in text are located near the towns of Gateway and Manitou Springs, Colorado, respectively. **(B)** Digital elevation model (DEM) of the Gateway, Colorado region. Unaweep Canyon is interpreted as a glacially carved valley dating from the late Paleozoic and partially reburied; the Cutler Formation, exposed near Gateway, Colorado, is interpreted to have accumulated when Unaweep Canyon was occupied by ice. Inset: Geologic map of the dashed rectangle depicted on the DEM. **(C)** Cross-section (A-A′) depicting the variation in facies from (inferred) most proximal glaciolacustrine to distal proglacial fluvial. The latter is the focus in the text. Line A-A′ is shown on **(B)**.

alluvial systems, proglacial systems also demonstrate a down-system progression of facies (e.g., Zielenski and Van Loon, 1998; Zielenski and Van Loon, 1999). In the proximal part of the system (within 5 km of glacial terminus), gravel predominates with horizontal, low-angle, and planar stratification as the most common sedimentary structures (Boothroyd and Ashley, 1975; Boothroyd and Nummendal, 1978; Maizels, 1993; Maizels, 1997; Zielinski and Van Loon, 1998). With increasing distance downstream, sand predominates and trough cross-stratification and ripple cross-lamination become more important (Boothroyd and Ashley, 1975; Maizels, 1993; Maizels, 1997; Zielenski and Van Loon, 1998). Beyond the proximal part of the system, the depositional record more closely reflects a braid plain dominated by sand with only gravel in primary channels (Zielenski and Van Loon, 2003). This transition from gravel to sand (within a few tens or hundred meters of the mountain front; e.g., Dingle et al., 2021) is less obvious in proglacial systems, which tend to be deficient in the 1–10 mm grain size range (e.g., Maizels, 1989; Zielenski and Van Loon, 1998). Given these characteristics and the ambiguous character of proglacial facies, the best reflection of a proglacial influence on sediment transport is expected in the most proximal deposits. Accordingly, we focus here on facies from the proximal system.

As streams gain power during, e.g., flood conditions, transport capacity increases, enabling incorporation of more sediment into the flow. Flows then transition from a state wherein grains are entrained by turbulence to a state wherein a mix of sediment-suspension mechanisms prevails, such as fluid buoyancy, intergranular collision, and matrix strength (Smith, 1986; Smith and Lowe, 1991; Baas et al., 2011; Baas et al., 2016). The resultant deposits range from scour-and-fill successions to low- and high-density hyperconcentrated flood flow (HFF) deposits (Figure 3; Smith, 1986; Todd, 1989; Scott et al., 1995; Sohn, 1997). Flows with more sediment than water possess a yield strength that must be overcome before flow can begin (e.g.,

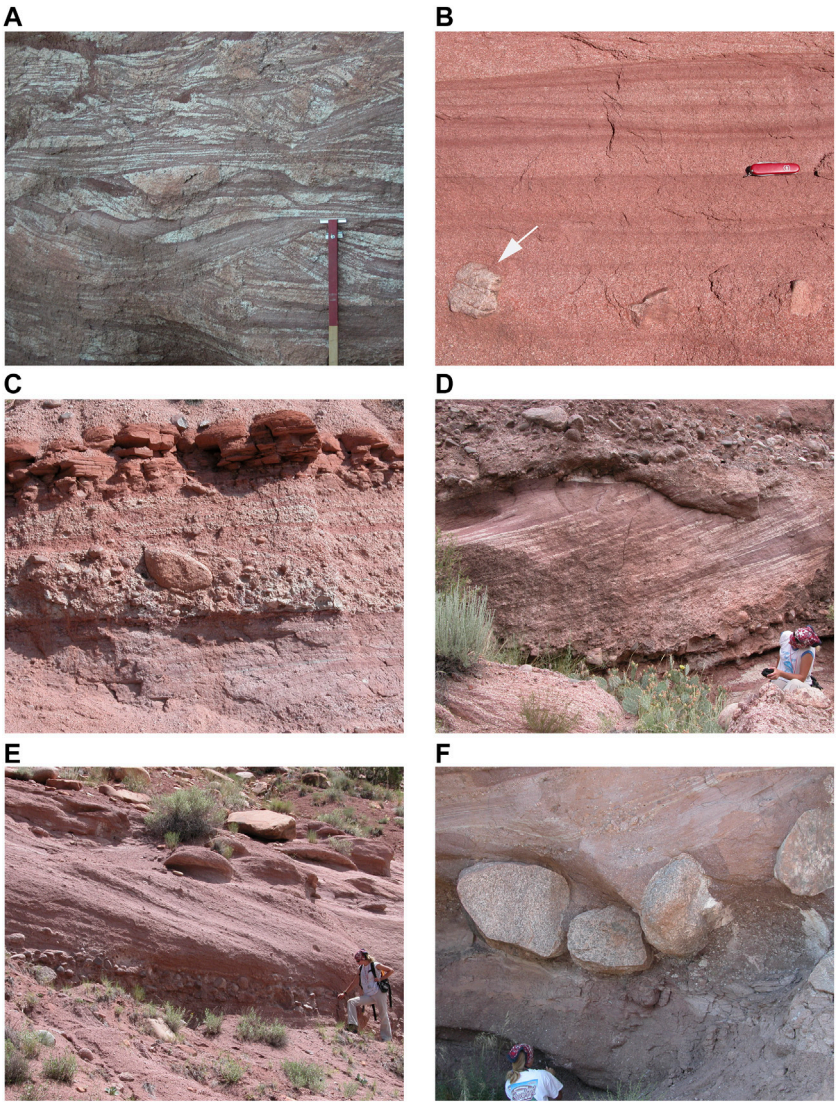

FIGURE 3
Photographs depicting a wide variety of facies observed in the Cutler system common to proglacial fluvial systems. **(A)** Scour-and-fill deposition of coarse-to granule-sized sandstone. Red component of Jacob Staff is 50 cm. **(B)** Low-concentration HFF deposit demonstrating horizontal and low-angle stratified sand and floating clasts. Floating clast indicated by white arrow is approximately 10-cm diameter. **(C)** High-concentration HFF demonstrating pulses of grading and outsized floating clasts (overlain by silt layer). **(D,E)** Large-scale cross bedding with foreset heights up to 2.5 m. This bed is traceable for at least 750 m along strike of the foreset dip. **(F)** Meter-scale boulders in a debris flow of the fluvial system. **(G)** Deposit demonstrating a hydrograph pulse where low-angle planar cross-stratification composes the base of the deposit, but transitions upward into high-concentration HFF deposit denoted by reverse grading and outsized clasts. Top of the bed exhibits normal grading and is capped by siltstone that drapes the unit. White arrow points to a ~15-cm diameter clast. **(H,I)** Deposits containing rip-up clasts of noncohesive fine sandstone and siltstone (white arrows). Inverse to normal grading apparent in **(I)**. **(J,K)** Pebbly mudstone deposits interpreted as cohesive fine-grained debris flows that underwent inflation during flow to reduce competency. See text for details. White arrow denotes a sandstone dike within the pebbly mudstone bed. **(L)** HFF with floating cobble in silt-sand matrix (snake for scale).

Pierson and Costa, 1987). These subaerial sediment gravity flows rely on fluid buoyancy, grain-to-grain collisions and/or matrix cohesion as sediment-support mechanisms. Thus, during flow evolution the grain size and sediment concentration evolve spatially and temporally and resultant deposits span the spectrum of flows with varying water saturations (cf. Pierson and Costa, 1987; Smith and Lowe, 1991). Here, we focus on deposits resulting from flows of either sediment-laden water or water-rich sediment that are most similar to the proximal proglacial systems described elsewhere (e.g., Maizels, 1997;

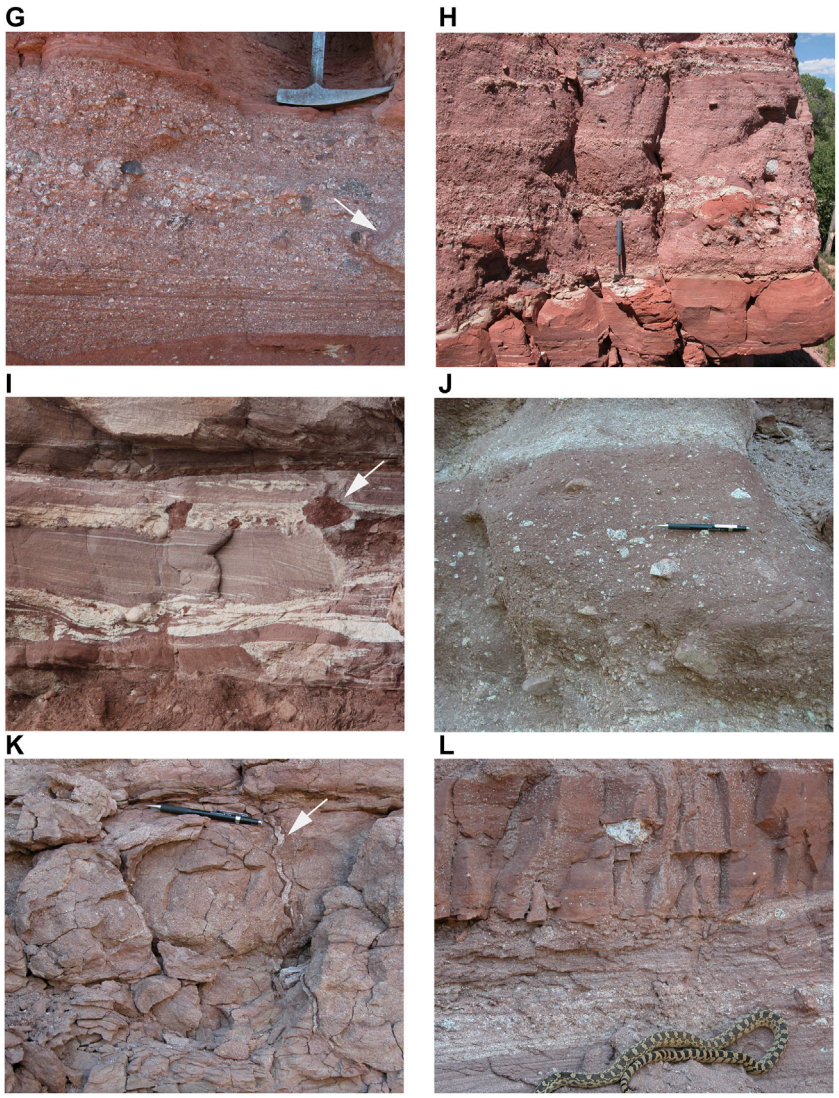

FIGURE 3
Continued.

Zielinski and Van Loon, 1998; Zielinski and Van Loon, 1999; Breien et al., 2008; Cui et al., 2010; De Blasio et al., 2011) and reflect terrestrial flow conditions between normal dilute stream flow and cohesive debris flow. Although not unique to proglacial fluvial systems, such mechanisms and resultant deposits are very common to proglacial systems, and thus can augment other observations indicating possible upland glaciation.

3.2.1 Scour-and-fill deposits

Streams with low sediment concentrations behave as Newtonian fluids, with turbulence providing the main sediment-transport mechanism (Smith, 1986; Pierson and Costa, 1987; Smith and Lowe, 1991). Under very low suspended sediment concentrations, a spectrum of lower flow-regime structures form, such as lower plane bedding and dune cross-stratification. With fine-to medium sand and moderate values of suspended clay (<~10%), current ripples and bed waves can occur; however, increased concentrations of suspended mud dampen turbulence (Baas et al., 2011). Initially, sand and gravel grains in suspension can enhance turbulence via grain-to-grain collisions, and turbulent wakes produced by flow separation around grains. With increasing sediment concentration, however, flow viscosity increases and grain-to-grain contact inhibits shear in the flow, which mutes turbulence (e.g., Bridge and Demicco, 2008). In this case, gravel deposits become more poorly sorted and prone to recording scour-and-fill structures rather than cross-stratification (Smith and Lowe, 1991). Proglacial systems transport large volumes of

suspended and bed-load sediment in braided-stream type systems (or "sandar" e.g., Marren, 2005), hence gravel and sand exhibiting scour-and-fill structures are common products of fully turbulent flows in proglacial systems (e.g., Maizels, 1993; Krzyszkowski, 2002).

Scour-and-fill structures also occur in other modern and ancient high-discharge systems such as ephemeral streams with seasonal or strongly intermittent discharge (e.g., Tooth et al., 2013; Priddy and Clarke, 2020). These deposits reflect abundant entrainable sediment during high-discharge events; however, in contrast to those from proglacial systems, ephemeral stream systems commonly have intercalated mud, intercalated calcretes on abandoned channels and floodplain deposits and/or the influence of eolian sand (Tooth et al., 2013; Priddy and Clarke, 2020). In some fluvial successions, scour-and-fill structures are commonly interpreted to record upper flow regime conditions (e.g., fast and shallow flows; Alexander et al., 2001; Fielding, 2006). In these cases, a sand-rich deposit exhibits cross-bedding that dips upstream, and laminae onlap a relatively deep (up to 0.75 m) scour surface. Moreover, in the case of chute and pool structures regularly spaced intervening highs are present (Fielding, et al., 2000; Alexander et al., 2001; Fielding, 2006). Scour-and-fill structures from proglacial and ephemeral streams may locally record these upper flow regime characteristics, but commonly do not (Smith and Lowe, 1991; Maizels, 1993; Priddy and Clarke, 2020), presumably because the discharge conditions during flooding events produce average flow depths that limit upper flow regime conditions.

3.2.2 Hyperconcentrated flood flow deposits

Hyperconcentrated flood flow (HFF) deposits were initially defined to record non-Newtonian flows with little-to-no strength where at least two sediment-support mechanisms prevail; these are intermediate between dilute stream flow and debris flow processes (Beverage and Culbertson, 1964; Pierson and Scott, 1985; Smith, 1986; Scott, 1988; Smith and Lowe, 1991; Zielenski and Van Loon, 1998; Sohn et al., 1999; Pierson, 2005). Somewhat later, the term hyperconcentrated flow was used to define flow with abundant suspended sediment concentration, such as within the Yellow River of China (Wan and Wang, 1994). Similar use of terms is confusing, but both terms largely describe a continuum of sediment transport processes with the term "hyperconcentrated flow" typically referring to flows with abundant suspended mud (up to ~25%) that reduces turbulence with increased sediment concentration (Wan and Wang, 1994; Baas et al., 2011; Baas et al., 2016). In contrast, HFFs indicate a higher sediment concentration (~25%–50% suspended material) where the role of turbulence as a sediment support mechanism subsides as fluid buoyancy and intergranular collisions begin to prevail (Beverage and Culbertson, 1964; Smith, 1986; Pierson and Costa, 1987; Smith and Lowe, 1991; Wan and Wang, 1994; Sohn et al., 1999). Moreover, suspended sediment in HFFs is recorded by the deposit itself and can range up to granule-sized, whereas deposits from hyperconcentrated flows are commonly the coarser substrate that interacts with the overlying mud-rich flow (Baas et al., 2011; Baas et al., 2016). HFFs capture a spectrum of sediment-water mixtures wherein fluid buoyancy and grain-to-grain collision work in the presence of turbulence at relatively low sediment concentrations (Smith, 1986; Smith and Lowe, 1991; Sohn et al., 1999) but yield to fluid buoyancy and grain-to-grain collisions as exclusive support mechanisms at higher sediment concentrations (Pierson and Scott, 1985; Scott, 1988; Sohn et al., 1999). Low-concentration HFFs result in sand- and granule-dominated deposits characterized by crude horizontal stratification and rare scours. Additionally, outsized clasts of cobbles and boulders are common in sand- and granule-rich HFF deposits, indicating sufficient buoyancy to support large clasts. Low-concentration, gravel-dominated HFF deposits are commonly graded and conspicuously lack lenses of stratified sand characteristic of normal stream-flow conglomerate deposits (Smith, 1986; Sohn et al., 1999). In contrast, high-concentration HFF deposits are predominantly sand-to pebble-sized and lack internal stratification except for graded (inverse to normal) sub-units within the deposit (Smith, 1986; Sohn et al., 1999). Elongate clasts can be oriented with long axes parallel to flow direction (Benvenutti and Martini, 2002). Similar deposits have also been inferred to reflect traction carpets, which result in graded beds or sub-units within a bed attributable to grain dispersion during the flow (e.g., Sohn, 1997; Sohn et al., 1999). Both low- and high-concentration HFF deposits are common in proglacial settings that emanate from mountain glaciers (e.g., Scott, 1988; Scott et al., 1995; Davies et al., 2003), valley glaciers descending from ice-fields (e.g., Lawson, 1982; Maizels, 1993), continental ice sheets (e.g., Shulmeister, 1989), and subaqueous glaciogenic fans (Brennand and Shaw, 1996). HFF flows have also been reported from temperate to arid alluvial fans, ephemeral fluvial systems, volcanic terranes, liquified landslides, and floods in mountainous regions (e.g., Bull, 1963; Beverage and Culbertson, 1964; Harrison and Fritz, 1982; Waitt et al., 1983; Ballance, 1984; Nemec and Steel, 1984; Pierson and Scott, 1985; Smith, 1986; Scott, 1988; Todd, 1989; Smith and Lowe, 1991; Best, 1992; Wan and Wang, 1994; Batalla et al., 1999; Sohn et al., 1999; Lirer et al., 2001; Benvenutti and Martini, 2002; Svendsen et al., 2003; Pierson, 2005; Kataoka et al., 2008; Calhoun and Clague, 2018). Thus, presence of HFF deposits should be used in combination with other features in assessing a glaciogenic origin.

3.2.3 Debris flows

Debris flows are non-Newtonian flows with yield (matrix) strength and high sediment concentrations. Owing to their common occurrence across a wide variety of depositional settings (both subaerial and subaqueous), stratigraphic, paleogeographic, and sedimentologic context is critical for interpreting their setting and significance. This discussion focuses on subaerial debris flows

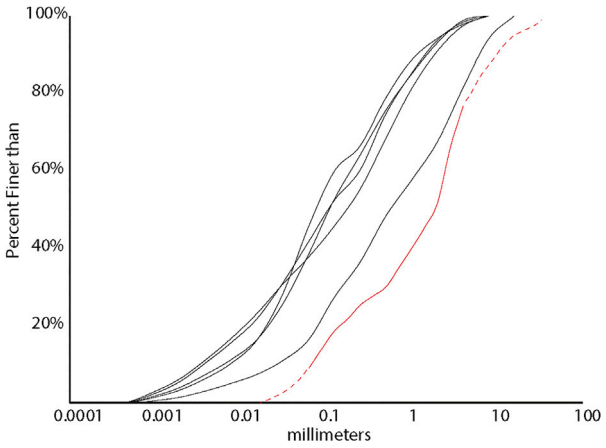

FIGURE 4
Cumulative grain-size distribution of fine-grained debris flows (black), and the fluvial facies from Soreghan et al. (2009; red) with dashed lines inferred to extend the distribution.

that experience rheologic transformation, as such flows are common in systems with either abundant entrainable sediment as well as abundant water in the system (e.g., Scott et al., 1995; de Haas et al., 2022)— conditions common to upland proglacial systems. On the other hand, rheologically stable flows produce common deposits in many systems, including alluvial and (nonglacial) fluvial systems, and mass flows in mountainous terrains.

Many upland glaciers exhibit debris flows with a wide variety of rheologic properties that vary spatially away from the glacier front. For example, Lawson (1982) observed active debris flows emanating from the Matanuska Glacier, AK (United States) that ranged from an internal plug with only basal shear, indicating high matrix strength (i.e., cohesive debris flows) to flows with the ability to raft clasts but also demonstrating significant vertical movement of sediment consistent with lower matrix strength (i.e., non-cohesive debris flows). Moreover, these flows commonly transformed from high-to low-strength matrix with the addition of water. Debris flows have also been observed to transform to HFFs with progressive incorporation of water (Pierson and Scott, 1985). In the Cascade Mountains of the Pacific Northwest (United States), Scott et al. (1995) inferred the opposite trend of flow transformation where the deposits emanating from glaciers show evidence of "bulking up" from normal stream flow to HFFs to non-cohesive debris flows. Through observational, experimental, and modelling studies, other workers have also demonstrated bulking of debris flows by addition of sediment from bank erosion after flow initiation from a glacial outburst flood (Breien et al., 2008; Cui et al., 2010; De Blasio et al., 2011). Downstream variation of flow events can also exhibit a spectrum of flow types from debris flow fronts to HFF tails (Scott et al., 1995; de Haas et al., 2022). Hampton (1972) and Hampton (1975) showed experimentally that competence of debris flows—a measure of the largest clast supported in the flow—reflects in part the relative abundance of water and the type of clay present. However, with increasing water, the sediment imposes a load on the fluid, and fluid buoyancy begins to support sediment in addition to matrix strength (Hampton, 1979). Taken together, these studies imply that subaerial debris flow deposits with characteristics attributable to rheologic flow transformation indicate environments with abundant entrainable sediment (leading to bulking) and water (leading to flow dilution) (Fisher, 1983). These conditions are common in proglacial environments (Scott et al., 1995; Cui et al., 2010, De Blasio et al., 2011), but are also common in various mountainous settings (e.g., Berti et al., 1999; Hungr and McDougall, 2005; de Haas et al., 2022) and in heavily forested and post-wildfire regions (e.g., Santi et al., 2008; Reid et al., 2016).

3.2.4 Outburst flood deposits

Seasonal flooding, as well as glacial lake outburst floods (GLOFs) are common in glacial systems, especially wet-based valley glaciers (e.g., Davies et al., 2003; Dessouki, 2009; Cui et al., 2010; Begam et al., 2018; Neupane et al., 2019). The rapid release of a large volume of water during outburst flood events produces a variety of deposits. For example, large bars can result in cross-stratification with foreset heights >1 m that extend laterally for hundreds of meters (Russell and Marren, 1999; Marren, 2002; Rushmer et al., 2002; Russell et al., 2005; Blazauskas et al., 2007; Benn and Evans, 2010). Deposits can record both the flow surge and its subsequent wane (Maizels, 1993). The surge is recorded by upward coarsening, massive to graded poorly structured sand and granule deposits, and HFFs (Maizels, 1993; Benn and Evans, 2010). Superjacent deposits recording decreasing flow conditions include trough cross-bedded sand and gravel, upward fining, normally graded sand, and crude horizontal stratification in sand and granule deposits (Maizels, 1989; Maizels, 1993; Maizels, 1997). Isolated pools of stagnant water can form in the latest stages of the waning flood, enabling suspension settling to form mm-to cm-thick mud drapes (e.g., Benn and Evans, 2010). Failure of natural dams—resulting from landslide or volcanic blockage of a drainage system (Fenton et al., 2006; Kataoka et al., 2008; O'Connor et al., 2009; Xiangang et al., 2017; Liu et al., 2019)—can produce similar deposits. However, relative to dam failures, proglacial systems are more likely to record repetitive occurrences of these high water-volume flood deposits because glacial meltwater is highly seasonal, resulting in abrupt discharges (e.g., Dessouki, 2009).

3.2.5 Case study: Proglacial fluvial sedimentation in the Pennsylvanian-lower Permian Cutler Formation (CO, United States)

Above, we focused on quartz grain microtextures in the Pennsylvanian-Permian Cutler Formation where exposed in their most uplift-proximal location (Case Study 3.1.1); but we

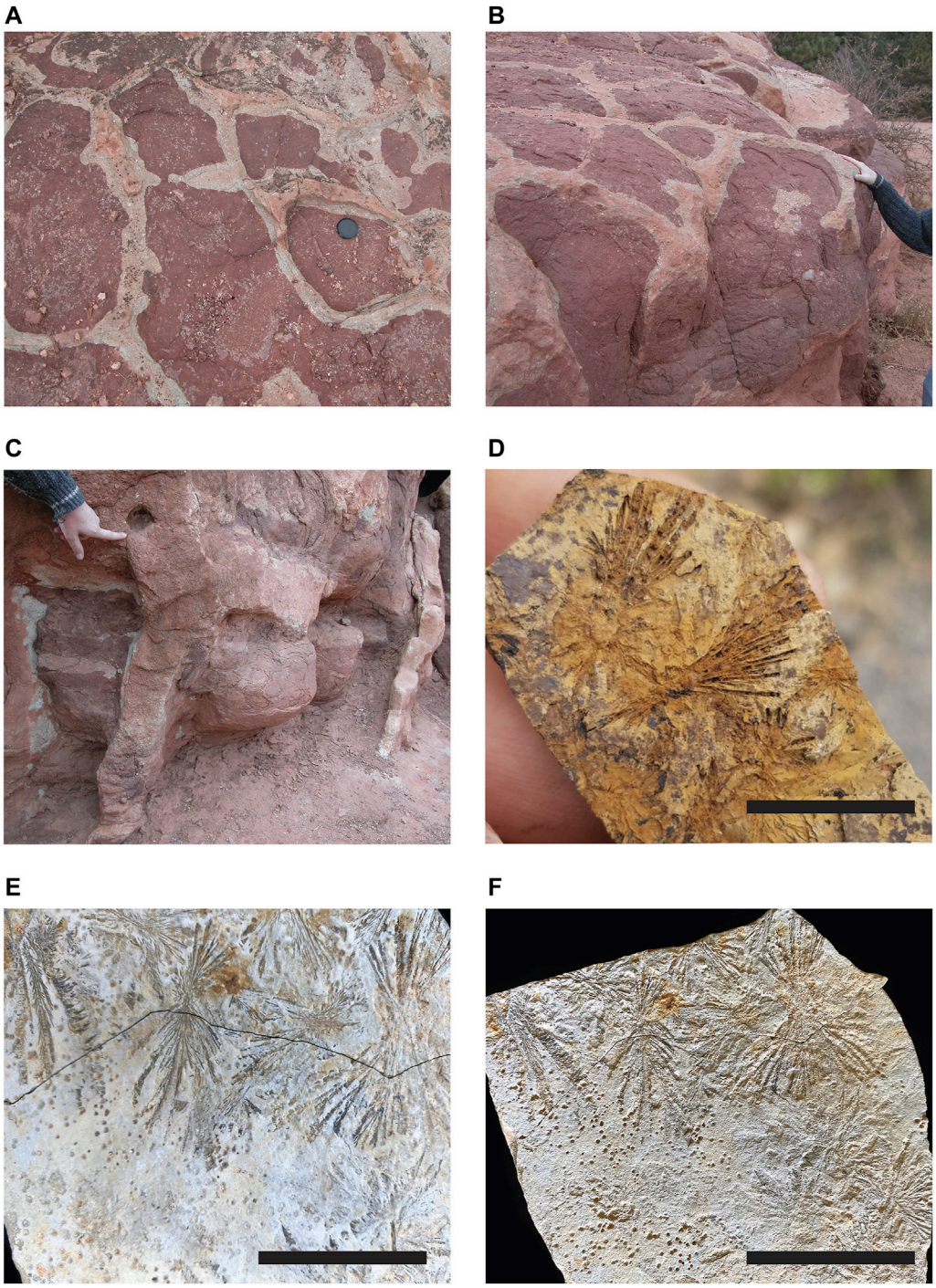

FIGURE 5
Inferred frozen ground phenomena (see Sweet and Soreghan, 2008) including **(A,B)** small-scale (20–75 cm) polygon interiors bounded by a polygonal fracture network in sand-rich substrate in the Pennsylvanian Fountain Formation, Colorado, **(C)** inferred frost wedging from the Fountain Formation, and **(D–F)** ice crystal casts from the lower Permian Usclas Formation, France (see Pfeifer et al., 2021). All scalebars are 1 cm.

hypothesize that fluvial deposits here also demonstrate glacial influence, owing in part to the predominance of granule-to-cobble dominated strata recording flows with inferred high sediment concentration and abundant water. The larger context is also critical (Figure 2): Proximally, these deposits onlap a paleovalley carved in Precambrian basement of a

paleo-uplift (the Uncompahgre uplift), and the most-proximal strata comprise hypothesized proglacial lacustrine facies exhibiting inferred dropstones, Gilbert-delta-like topsets and foresets, and boulder-to granule subaqueous mass flows deposits (Moore et al., 2007; Soreghan et al., 2009). Dilute stream-flow deposits with dune structures here are quite rare, similar to other proximal proglacial settings (Maizels, 1993; Zielenski and Van Loon, 1998), and most cross-strata are low-angle and best characterized as scour-and-fill deposits (Figure 3A). HFF deposits are common to the Cutler system, typically as crudely stratified coarse to very coarse sand- and (predominantly) granule deposits with outsized floating clasts (Figures 3B,C) indicating that both fluid buoyancy and turbulence acted as sediment support mechanisms. One instance of high-angle cross-stratification is noteworthy in that the foresets approach 2 m in height and extend laterally for at least 750 m (Figures 3D–F; Soreghan et al., 2009), recording a major flooding event—analogous to the large prograding bars observed during GLOFs (e.g., Marren 2002; Blazauskas et al., 2007). Rip-up clasts of underlying non-cohesive (fine sand) material are commonly incorporated into these HFF deposits (Figures 3G,H), which appear analogous to rip-ups of frozen bank material depicted in Diffendal (1984). Numerous occurrences of stacked facies demonstrate the rise and fall of flood hydrographs (Soreghan et al., 2009). For example, rare lower flow regime dune deposits are locally overlain by reverse graded granule deposits inferred as high-concentration HFFs (Figure 3I). These in turn are commonly overlain by crudely stratified granule deposits reflecting a low-concentration HFF deposit. This progression of stacked facies suggests normal stream conditions evolved to high-concentration HFF conditions as the flood event hydrograph peaked, and then on the falling limb of the hydrograph, low-concentration HFF conditions prevailed. Comparatively, deposits in fluvial systems and experiments with hyperconcentrated silt and clay in suspension in fully turbulent conditions exist up to a concentration of about 8% suspended mud, but with increased sediment concentration turbulence is progressively muted and then fully suppressed by about 25% suspended concentration (e.g., Baas et al., 2011; Baas et al., 2016). Abundant granule deposits are not consistent with such conditions. Locally, laminated siltstone overlies these facies, which may indicate deposition from an isolated pond that formed after the flood subsided (e.g., Benn and Evans, 2010). Figure 3 depicts the wide variety of facies associations observed in this system and commonly demonstrate changing flow conditions within the same deposit.

Flow transformation can also be inferred from some deposits. For example, deposits with abundant granule-sized grains in a muddy matrix (Figures 3J,K) are inferred to record cohesive fine-grained debris flow deposits (Sweet, 2017). However, these deposits uniformly lack the larger cobbles and boulders otherwise pervasive within the system (Figure 4), indicating the action of a mechanism to rid the flow of the larger clasts. The simplest explanation is flow inflation by ~ 60% through the incorporation of water after the flow initiated to account for the loss of competence (Sweet, 2017), similar to debris-flow transformations in modern proglacial systems (Lawson, 1982; Pierson and Scott, 1985; Scott et al., 1995). These fine-grained debris-flow deposits indicate the ready availability of abundant water, given the persistent occurrence of these deposits in the studied stratigraphic succession (Soreghan et al., 2009; Sweet and Soreghan, 2010b). Moreover, the deposits are common to other coeval strata regionally indicating that they were an important process acting in the late Paleozoic uplift-proximal alluvial systems of Colorado (Sweet and Soreghan, 2010b).

Previous authors viewed the crude bedding, inferred fluvial and sediment-gravity flow facies of the Cutler system, and its position adjacent to a paleouplift to argue for alluvial-fan deposition (Mallory, 1958; Elston and Shoemaker, 1960; Baars, 1962; Cater, 1970; Werner, 1974; Mack, 1977; Campbell, 1979, Campbell, 1980; Mack and Rasmussen 1984; Schulz, 1984), and—indeed—many types of flows, including HFFs and debris flows are common to non-glacial alluvial and fluvial systems. Some (Campbell, 1979, Campbell, 1980) argued specifically for a hot-humid fan, whereas others (Mack, 1977; Mack and Rasmussen, 1984) argued for a hot-arid fan. But signs of subaqueous deposition for the proximal-most mass flow deposits (Shultz, 1984; Soreghan et al., 2009), in addition to the large-scale bar deposits recording abundant water in the fluvial system—yet relatively low chemical weathering—hint at alternative interpretations. The proglacial—or cold-humid—interpretation advocated by Soreghan et al. (2009) emanates in part from consideration of facies analyses indicating that the proximal-most Cutler system represents a lacustrine environment complete with inferred dropstones and dump structures near its onlap contact with Precambrian basement of the paleo-uplift. Furthermore, it fills a small paleovalley visible in outcrop that leads into Unaweep Canyon, an inferred glacial paleovalley dating from the late Paleozoic (Soreghan et al., 2007; Soreghan et al., 2008b). These associations, taken together with the common occurrences of faceted clasts in the proximal Cutler and widespread paleo-loess in the distal Cutler (Murphy, 1987; Soreghan et al., 2002) support a proglacial interpretation for this system.

3.3 Frozen ground phenomena

Cold-weathering phenomena, such as polygonal cracking of sand-rich sediment (e.g., Lachenbruch, 1962; Black, 1976), or preservation of ice-crystal impressions in fine-grained sediment, are common in modern periglacial environments. But direct evidence of freezing temperatures (even ephemeral freezing) in the ancient record can have significant implications for paleoclimate reconstructions. For example, the recent

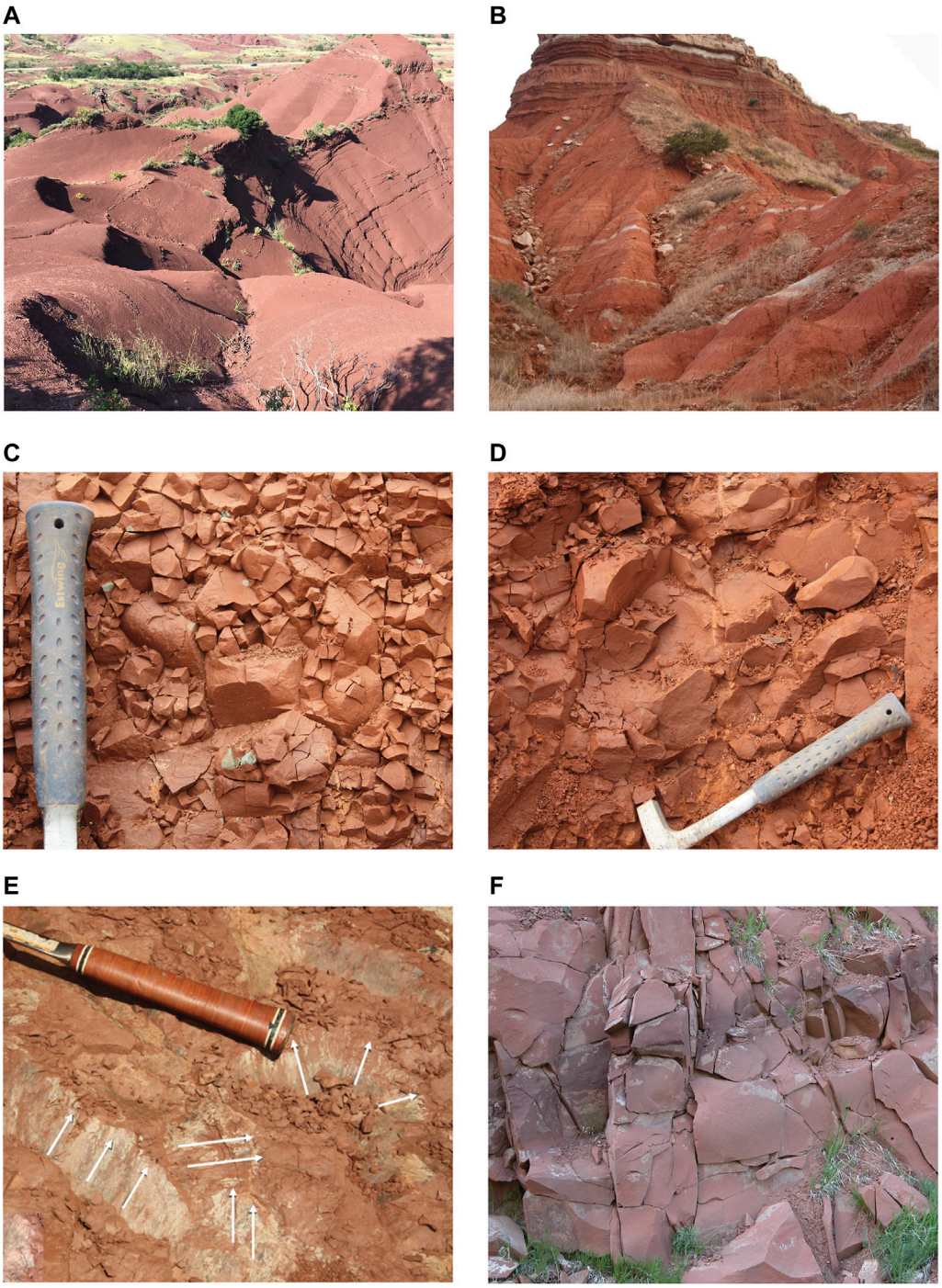

FIGURE 6
Macromorphological (outcrop-scale) attributes of loess and eolian-transported dust including **(A,B)** massive, structureless bedding from the Permian Salagou (France) and Flowerpot (OK, United States) formations, **(C,D)** blocky-to-angular fracturing from the Permian Dog Creek Formation (OK, United States), and **(E,F)** pedogenically-altered loessite from the Maroon (CO, United States) and Salagou (France) Formations.

documentation of low-latitude, low-elevation ice-crystal impressions and frozen ground features from the late Paleozoic record of eastern and western equatorial Pangea (Figure 5; Sweet and Soreghan, 2008; Pfeifer et al., 2021; Voigt et al., 2021) require much colder temperatures than typically assumed for low-elevation equatorial paleolatitudes.

Bedding-plane traces of ice crystals (pseudomorphs) that record at least intermittent freezing of water-saturated sediment are recognized in the geological record from the Ordovician (Morocco and Libya; Nutz et al., 2013; Girard et al., 2015) to the Pleistocene (United States; Mark, 1932; French and Shur, 2010) and in several intervening intervals (e.g., Clarke, 1918; Udden, 1918; Lang et al., 1991), with the largest incidence of low-latitude ice-crystal impressions dating exclusively from the upper Carboniferous—lower Permian [Germany, France, New Mexico, and Colorado (Lang, 1937; Reineck, 1955; Pfeifer et al., 2021; Voigt et al., 2021)]. Laboratory-simulated features that mimic the impressions left by the freezing of water-saturated mud (Allan, 1926; Mark, 1932; Reineck, 1955; Pfeifer et al., 2021) support interpretations of ice crystal molds in the ancient record. The morphologies of these enigmatic features can resemble rare forms of saline minerals (e.g., gypsum, halite, barite), and thus might be overlooked as ice-crystal traces, but ultimately the strong resemblance to ice crystal impressions in modern mudflats (in scale and form) supports ice crystal growth as the primary mechanism of formation (Figure 5D–F; Pfeifer et al., 2021).

3.3.1 Case study: Frozen ground phenomena in the upper Pennsylvanian Fountain Formation

A polygonal network of fractures occurs in Pennsylvanian strata of the Fountain Formation along the Front Range of Colorado (proximal to the ancestral Front Range; Figures 5A,B). The fractures occur in two discrete intervals and at two different scales. The interior polygons <75 cm in diameter for the smaller set are observable in outcrop, while the larger set is 10 s of meters in diameter and inferred based on variably oriented deeply penetrating cracks (Sweet and Soreghan, 2008). At each locality, the cracked substrate is massive (structureless) with sand and granule volume ranging from 70% to 95%. Cracks taper downward from the top of the paleosol horizon and penetrate more deeply (typically 2–3 m) for larger polygons (Sweet and Soreghan, 2008).

Polygonal cracking observed within paleosol intervals is most commonly attributed to desiccation of a muddy substrate; however, a desiccation origin is untenable where the substrate comprises non-cohesive sediment such as sand and/or granules (e.g., 50%–88% sand precludes crack development in various experiments; Fellows, 1951; Neal, 1978; Kleppe and Olsen, 1985; Weinberger, 2001). In the Fountain Formation, the granulometry of the substrate precludes desiccation (e.g., mud cracking) as an explanation, and the host lithology and characteristics similarly preclude the operation of other binding mediums (e.g., evaporites, fossil algae) that could impart the volume change needed to facilitate cracking (Sweet and Soreghan, 2008). Thus, these features are inferred to represent frozen ground that underwent volume change due to diurnal and seasonal temperature swings, producing the polygonal network of cracks. Thermal cracking of frozen soils occurs when already frozen ground is subjected to further cooling (Lachenbruch, 1962; Mackay, 1974; Maloof et al., 2002). Thus, if the polygonal cracks in the Fountain Formation are the result of thermal cracking of frozen ground, then the features record at least seasonally frozen ground conditions.

3.4 Loess and eolian-transported dust deposits

3.4.1 Definition and origin of loess deposits

Loess refers to wind-transported continental deposits of predominantly silt size (Muhs et al., 2003; Muhs et al., 2013) and composed largely of quartz, feldspars, and clay minerals (Muhs et al., 2003). By outcrop area and volume, loess is the most abundant terrestrial deposit for the Quaternary (Catt, 1988), covering about 6% of land area today (Li et al., 2020b); many authors consider loess particularly characteristic of the Quaternary (e.g., Catt, 1988; Smalley, 1995; Muhs et al., 2003; Li et al., 2020b), for reasons explored further below.

Although the eolian origin of loess is well established, the genesis of the silt-sized material has been long debated. (Tutkovskii, 1899; in Smalley et al., 2001) was the first to suggest a link between loess and glaciation, a view subsequently echoed (e.g., Smalley, 1966; Smalley, 1995; Smalley et al., 2001), and demonstrated in part by the abundant silt content of subglacial till (Boulton, 1979), as well as the close spatial and temporal association between (former) glaciation and loess deposits (Catt, 1988; Smalley, 1995).

The efficacy of glacial grinding as a silt-production mechanism is now unequivocal, but significant debate has lingered regarding the possible role of other, non-glacial processes in silt production, particularly the role of intergranular collisions during eolian saltation. Whereas Kuenen (1960) found this to be an ineffective means of silt production, subsequent studies suggested the opposite (e.g., Whalley et al., 1987; Smith and Lowe, 1991; Wright et al., 1998; Wright, 2001; Bullard et al., 2004; Bullard et al., 2007; Enzel et al., 2010). However, more recent studies (Swet et al., 2019; Adams and Soreghan, 2020) designed to realistically test the capacity of saltation-induced grain fracturing as a silt production method showed negligible silt production, reinforcing Kuenen's (1960) original conclusions. This, and the absence of significant loess surrounding large deserts (e.g., Sahara and Australian deserts; Smalley and Krinsley, 1978; Smalley, 1995) call into question the efficacy of hot-desert processes for primary silt production in the "loess mode" variously defined as 20–50 μm (Smalley and Krinsley, 1978) or 20–30 μm (Tsoar and Pye, 1987; Assallay et al., 1998). Rather, desert regions with significant loess are invariably associated with distal glaciated mountains (Smalley and Krinsley, 1978; Smalley et al., 2009; Li et al., 2020).

The manufacturing of silt-sized material from non-silty protoliths requires comminution, an energy-intensive process readily achieved in the subglacial environment (Smalley, 1995; Assallay et al., 1998). The other way to easily generate abundant

TABLE 3 Particle size and mineralogy of selected loess deposits.

Location	Unit	Age	Climate	Mode (μm)	%QF	%Clays	%Carbs	References
Israel	Negev Loess	Q	D	50–60	46	20–55	35	Crouvi et al. (2008)
Canary Island	Loess	Q	D	5	53	<1	40	Menendez et al, (2007); Stuut et al. (2009)
Australia	Alluvial loess	Q	D	58	51	39	4	Haberlah et al. (2010)
United States	Peoria Loess	Q	G	24–56	~80	17	3	Winspear & Pye (1995); Muhs et al. (2018)
Poland	Zlota Loess	Q	G	NR	88	1	6	Kenis et al. (2020)
Switzerland	Loess	Q	G	16–30	84	NR	NR	Martgnier et al. (2015)
United Kingdom	Smith Bank Fm	Tr		30–50[a]	55	35	7	Wilkins et al. (2018), Wilson et al. (2020)
United States (UT)	Ankareh Fm	Tr		30–45[a]	45	27	27	Chan, (1999)
France	Salagou Fm	P		17[a]	60–70	20–30	NR	Pfeifer et al. (2016), Pfeifer et al. (2021)
United States (OK)	Dog Creek Fm	P		15–50	NR	NR	NR	Foster et al. (2014); Soreghan et al. (2015)
United States (CO)	Maroon Fm	P		30–35[a]	95	NR	NR	Johnson (1989); Soreghan et al. (2008a)

QF, non-clay silicates (mostly quartz and feldspars); Clays, phyllosilicates and Carbs, carbonates, all reported in relative percent. Age: Q, Quaternary; Tr, Triassic; P, Permian. For Quaternary loess, Climate refers to the inferred origin in desert (D) or glacial (G) regions.
[a]In modes indicates 2D analysis of lithified samples.

silt is to liberate it from precursor lithologies composed of ready-made silt, such as siltstone, volcanic ash (tuff), or fine-grained metamorphic rocks such as phyllite (Kuenen, 1960). Alternatively, silt and clay can be deflated from dry lake beds, such as the diatom-rich silt emanating from the Bodélé Depression, termed by some the "dustiest place on Earth" (Washington et al., 2006; Bristow et al., 2009).

Smalley and Derbyshire (1990) proposed the term "mountain loess"—meaning loess produced by cold-climate processes in mountains—as distinct from "glacial loess"—that produced by continental glaciation, and posited these as the two main sources for making the silt that forms loess. In a recent compilation of loess occurrences globally, Li et al. (2020b) advocated for classification of loess genesis into three modes as follows:

1) Continental glacier-river transport (CR) mode—produced by low-elevation continental glaciers and transported to lower reaches of rivers for deflation. Examples include the large loess regions of the central United States and eastern Europe.
2) Mountain-river (MR) mode—produced by high-altitude areas and transported to lower reaches of rivers for deflation. For this mode, river transport ranges from 200 to 600 km (but up to 1,000 km), with loess deposits occurring within ~50–300 km of the middle-lower reaches of the river. Examples include loess deposits associated with the Alps, Altai Mountains, Alaska Range, and the Andes.
3) Mountain-river-desert (MRD) mode—produced in high-altitude areas then transported by rivers to their middle-lower reaches, or to desert basins, from which they can be subsequently deflated. For this mode, the average eolian transport distance from the rivers to the centers of loess accumulation can exceed 700 km. Examples include the Chinese Loess Plateau (the single largest loess deposit today) and the Negev Loess in Israel (relatively thin). Thick accumulations of MRD-mode loess are all associated with glaciated mountain regions, whereas thin or discontinuous MRD-mode loess deposits are not (e.g., sub-Saharan loess, Negev loess).

All three loess modes (CR, MR, MRD) include the potential influence of glaciers within the "zone of production," although some amount of transport in rivers is also characteristic (Smalley, 1995; Smalley et al., 2009). On balance, a century of study on the origin of loess suggests that large volumes of the requisite (silty) material are most easily produced by glacial grinding (continental and mountain), albeit mountain weathering (cold climate, including glacial) processes can play important roles as well. The close empirical association with glaciation provides a means to consider loess as a proxy for glaciation, as explored further below.

3.4.2 Paleo-loess (loessite) as a potential indicator of glaciation

Common attributes of paleo loess, or loessite (Figure 6) include thick (up to several-meter "beds"), laterally continuous and structureless (massive) siltstone that commonly exhibits pedogenic features or horizons, but neither grain modes that exceed the silt size, nor channelization (Johnson, 1989; Soreghan et al., 2008a). An absence of alternative explanations for delivery of the sediment (e.g., absence of fluvial features) strengthens an interpretation of eolian delivery. Loessite has also been identified in core, based primarily on documentation of massive (unstructured), monotonous siltstone (e.g., Kessler et al., 2001; Dubois et al., 2012; Giles et al., 2013), and random grain-fabric orientations (Wilkins et al., 2018). Sedimentary structures (e.g., ripples, desiccation cracks, laminations) are common in silt-rich strata otherwise posited to record eolian delivery, indicating reworking by water or pedogenic processes (Johnson, 1989;

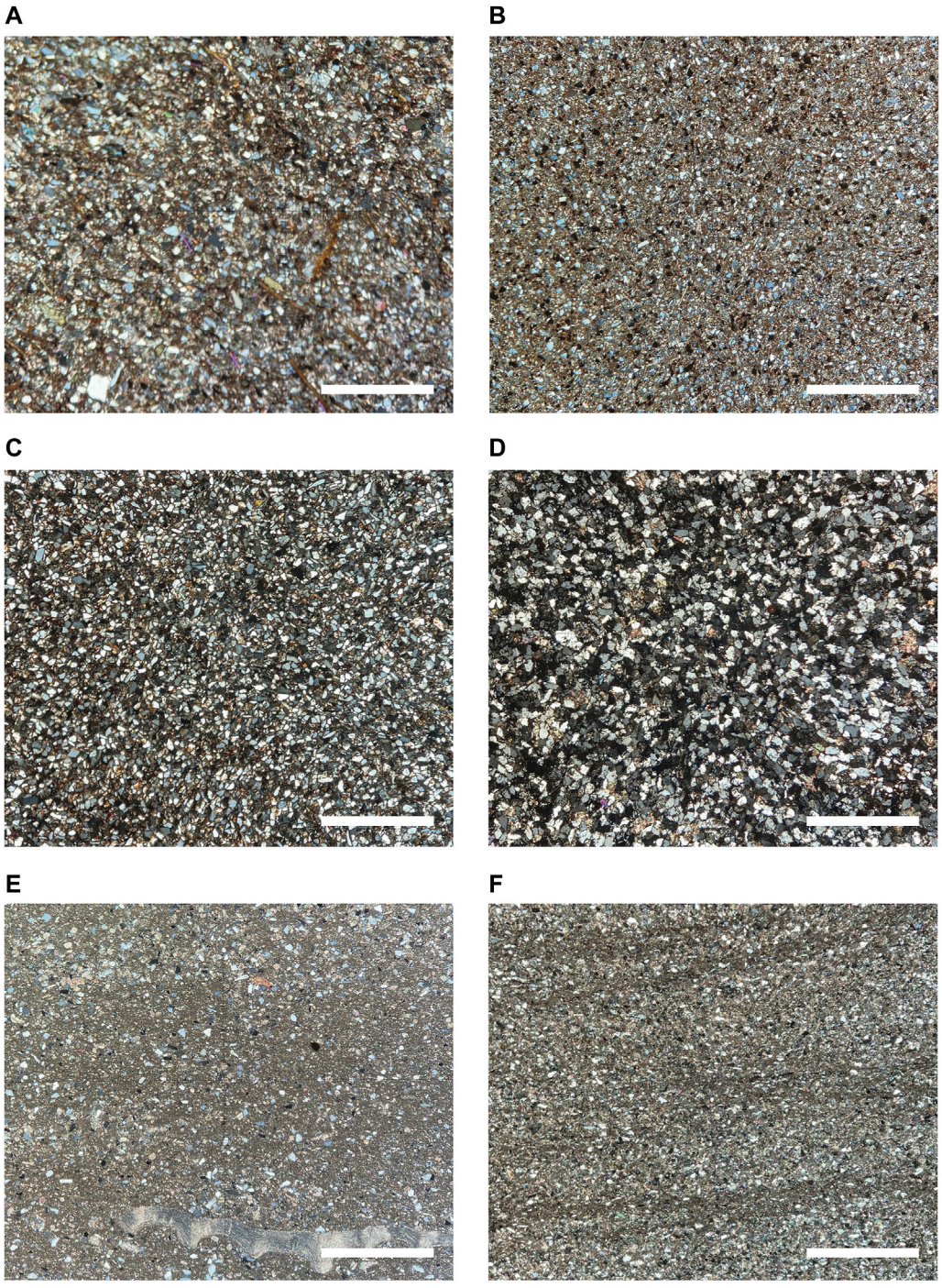

FIGURE 7
Micromorphological (thin section) attributes of loess and eolian-transported dust in assorted Upper Pennsylvanian-Permian formations in the western United States including **(A,B)** proximal and distal Cutler Formation loessite (Colorado and Utah, respectively), **(C)** Tubb Formation loessite (New Mexico), **(D)** Maroon Formation loessite (Colorado), and **(E,F)** quartz silt (dust) in the marine Naco Formation (Arizona). All scalebars are 2 mm.

Soreghan et al., 2008b; Giles et al., 2013; Sweet et al., 2013; Foster et al., 2014; Wilkins et al., 2018; Pfeifer et al., 2020), since wet surfaces enhance dust trapping.

Loess is a well-known paleoenvironmental proxy, for parameters such as paleoatmospheric circulation (wind regimes; Vandenberghe, 2013), and hydroclimate (e.g.,

paleoprecipitation; Maher, 2016). Until relatively recently, loess was recognized exclusively from the Quaternary record, and linked in part to the widespread icehouse conditions of the Quaternary; but now paleoloess has been recognized in Earth's deep-time record, especially from the Carboniferous-Permian icehouse (Murphy, 1987; Johnson, 1989; Kessler et al., 2001; Mack and Dinterman, 2002; Soreghan et al., 2002; Tramp et al., 2004; Soreghan et al., 2007; Soreghan et al., 2008a; Giles et al., 2013; Sweet et al., 2013; Foster et al., 2014; Soreghan et al., 2014; Pfeifer et al., 2020), and the Neoproterozoic icehouse (Edwards, 1979; Retallack, 2011; Retallack et al., 2015). But a few examples of inferred Mesozoic (mostly Triassic; one Cretaceous) loessite (Chan, 1999; Jefferson et al., 2002; Lawton et al., 2018; Wilkins et al., 2018; Wilson et al., 2020) exist, deposited during greenhouse intervals, which calls into question what if any attributes of loess might specifically indicate a glacial genesis. We hypothesize that, under certain circumstances the recognition of loess exhibiting particular attributes can raise the hypothesis of glaciation contemporaneous with loess deposition.

Assallay et al. (1998) noted that loess occurring in warm desert regions typically exhibits primary modes either finer (2–4 μm) or coarser (60–125 μm) than the "typical" primary loess mode (wherein >50% of the sediment is 10–50 μm; cf. Browzin, 1985). Crouvi et al.'s (2008) review of warm-desert loess deposits reinforces this, citing coarse medians (58–80 μm) and both very fine and coarse modes (multiple: 3–8 μm, 5–20 μm, 50–100 μm). In contrast, examples of classically glacial (Quaternary) loess deposits display primary modes that typically range between ~25 and 50 μm (Table 3). Moreover, a literature review indicates that clay and/or carbonate content of warm-desert loess units tend to be significantly higher than those reported from glacial loess, which is dominated by primary minerals (Table 3).

The few examples of paleo-loess deposits from deep-time intervals lying outside of icehouse climates, and for which relevant data exist, indeed commonly exhibit relatively fine modes (<10 μm), and high clay mineral (27–35%) and/or carbonate (up to 27%) contents, albeit the carbonate present in deep-time examples could be purely diagenetic (Table 3). For example, Wilkins et al. (2018) interpreted the Smith Bank Formation (Triassic, United Kingdom) as loessite, but documented a significant component of silt-sized clay pellets sourced from desiccation of lacustrine systems, and correspondingly abundant clay mineral content (~35%). Furthermore, Wilson et al. (2020) showed that the sources for this loessite comprise primarily fine-grained precursors, such as sedimentary, and basic and acid-intermediate magmatic and volcanic lithologies. Similarly, the Mercia Mudstone (Triassic, United Kingdom) is interpreted to comprise silt-sized clay agglomerates, akin to the "parna" of Australia, which is reflected in the high (70) values of the Chemical Index of Alteration (CIA) of these strata (Jefferson et al., 2002; Mao et al., 2021). Chan (1999) reported relatively coarse size modes (estimated 30–45 μm by thin section analysis) for the Ankareh Formation loessite (Triassic, United States), but high clay and carbonate contents (27% each; Table 3). Finally, Chen et al. (2019) inferred "loess" or far-travelled dust from deposits exhibiting primary modes of ~3 μm (Cretaceous, China).

In contrast, paleo-loess reported from many units of the Carboniferous-Permian (Table 3) exhibit modal grain sizes (silicate fraction) generally in the 15–40 μm range, predominantly (>80%) primary silicate mineralogical compositions (with minimal clays, biogenic material, or carbonate phases), and evidence for minimal chemical weathering (e.g., low CIA values; e.g., Nesbitt and Young, 1982; Soreghan et al., 2008a). Despite the challenges in reconstructing accurate volumes, measured sections document anomalously thick (10 s to >1000 m) and widely distributed accumulations of loess deposits from this time interval—including the thickest (700 m to >1.5 km) loess deposits yet documented from any time or place in Earth history (Soreghan et al., 2008b; Pfeifer et al., 2020). Given these examples, we hypothesize that paleo-loess can be an indicator for glaciation when it exhibits many or most of these attributes. Used in combination with provenance data, these attributes can support a hypothesis of silt generation via glacial grinding (e.g., if protoliths for the silt-sized material are predominantly coarse-grained igneous and metamorphic units—see Case Study 3.4.4). In summary, (paleo) loess exhibiting 1—primary size modes of ~15–50 μm and provenance data indicating derivation from (mostly) non-silt precursors, 2—a significant fraction of primary silicate minerals and relative dearth of clay, and 3—evidence for relatively minimal chemical weathering, such as CIA values similar to the source rock(s), signals the probability of silt generation by glacial grinding. The case is strengthened further given large volumes of material, and evidence for possible pulsed dust deposition, with greater flux during inferred glacials relative to interglacials (M. Soreghan et al., 2014). However, once made, silt is readily recycled. Hence the need to combine observations from multiple attributes to narrow the interpretation.

3.4.3 Eolian-marine strata signaling silt generation

Given the reasoning above, we hypothesize that preservation of widespread loess in Earth's past can signal glaciation contemporaneous with loess (ite) deposition. For intervals of Earth history when glaciation occurred, but epeiric seas predominated across lowland regions, however, the proxy for abundant silt generation might be preserved in epeiric sea deposits—not as loess, but as eolian-transported marine strata.

Upper Devonian (Fammenian) through Permian strata of a growing number of regions, especially in the US mid-continent

TABLE 4 Summary assessment of proxies discussed in this paper.

Proxy	Strength	Weakness
High-stress quartz microtextures (grooves, troughs)	Strong correlation with generation in proximal (<50 km, up to ~200 km) glacial systems	Also present in fluvial/eolian deposits where recycled from glacial systems. Frequency of occurrence varies by glacial system (ice thickness)
Scour and fill deposits	Produced by fully turbulent flows in proglacial systems. More typical of proglacial where deposits lack upper flow regime characteristics or intercalated mud/eolian sand	Common across a variety of high-discharge depositional settings (including non-glacial)
Hyperconcentrated flood flow deposits	Both low- and high-concentration HFF deposits are ubiquitous in proglacial systems	Common across a variety of depositional settings (including non-glacial)
Subaerial debris flows (w/rheologic transformation)	Especially common in proglacial systems owing to abundant water and entrainable sediment	Common across a variety of depositional settings (including non-glacial)
Outburst flood deposits (seasonal)	Common in proglacial systems, especially wet-based valley glaciers, owing to seasonal and subglacial melting and impounding	Failure of natural dams can produce similar deposits
Frozen ground phenomena	Demonstrates at least seasonally- diurnally cold temperatures conducive to glaciation	Consistent only with temperatures that can enable glaciation; no correlation to proximity of glaciation
Loess (ite) and eolian-transported dust	Strong empirical association between wet-based glaciation and silt production, large loess deposits	Silt occurs in non-glacial systems

contains a remarkably rich record of marine silt- and mudstone inferred to reflect eolian transport (Soreghan et al., 2008b; McGlannan et al.[1]). The most straightforward examples of eolian-transported siliciclastic material are those preserved within carbonate buildups or carbonate platforms that formed (paleo) geographically isolated—or at least far removed—from fluvio-deltaic source regions (e.g., Soreghan et al., 2008a; Sur et al., 2010; Carvajal et al., 2018; Oordt et al., 2020; Sardar Abadi et al., 2020; McGlannan et al.). Attributes that signal eolian transport include 1—grain-size modes predominantly in the silt fraction, although these can skew toward the fine to lower-medium silt sizes in cases of longer transport distances (c.f. McGlannan et al.), 2—blanket-like distribution over wide regions, and 3—absence of nearby fluvio-deltaic or submarine-fan feeders or other explanations for siliciclastic incursions. As above, attributes that signal a possible glacial derivation include a large volume/wide distribution, low clay-mineral content (and thus correspondingly low chemical alteration, such as low aluminum content), and provenance from known uplands that exposed silt-poor protoliths.

3.4.4 Case study: Loess of the Permian Salagou Formation (Southern France)

Pfeifer et al. (2020) interpreted the Salagou Formation—a ~1.5 km-thick monotonous section of fine-grained Permian redbed strata preserved in the intramontane Lodève Basin (south-central, France)—to record eolian transport and deposition as loess. Despite its now well-lithified and diagenetically altered state, the interpretation as paleoloess is based on sedimentological characteristics (detailed facies and petrographic analysis), quantitative grain-size analysis, geochemical analysis that reflects a low degree of chemical weathering, provenance data that indicates the action of comminution to reduce grain size from source to sink, and a lack of evidence for fluvial deposition or any other suitable mechanism for generating or delivering such a large volume of uniformly silt-sized sediment into the basin. Relative quartz grain-size analysis was possible using 2D backscatter electron (BSE) image analysis techniques and stereological corrections (e.g., Soreghan and Francus, 2004).

Sedimentological attributes that define this ancient loessite (Figures 6, 7) include 1) a predominance of massive (structureless) and homogeneous mudstone occurring in beds up to 15-m thick that fracture in a blocky-angular manner, 2) a silt-sized distribution of quartz in an illite-hematite-rich matrix, and 3) evidence for pedogenic overprinting at the macro- and microscale including 10+ cm randomly oriented semi-radial slickensides and abundant micromorphological attributes such as wedge-shaped peds, clay grain coatings, and other pedogenic fabrics.

Detrital zircon data from the Salagou Formation loessite (Pfeifer et al., 2016) record coarse-grained protoliths within the Montagne Noire core complex situated on the western margin of the Lodève Basin. Quantitative (2D) quartz grain-size analysis from known source lithologies in the Montagne Noire show that quartz size must have been reduced substantially—especially from the coarsest lithologies (granite), but even from the finest lithologies (schist)— to achieve the silt modes prevailing in the Salagou Formation. Furthermore,

1 McGlannan, A. J., Bonar, A., Steinig, S., Valdes, P., Pfeifer, L. S., Adams, S. An eolian dust origin for clastic fines of Devono-Mississippian mudrocks of the greater North American Midcontinent. J. Sediment. Res. In review.

geochemical proxies record a low degree of chemical weathering: CIA values of the Salagou Formation loessite (average 63) are consistently low and overlap with CIA values from known source rocks in the Montagne Noire (59–70).

These data are most consistent with physical (glacial and periglacial) weathering in the paleo-uplands as the primary mechanism by which to generate large volumes of silt-sized grains, ultimately reinforcing the interpretation of the Salagou Formation as an ancient loessite.

4 Discussion: Bolstering our understanding of paleoclimates with upland knowledge

4.1 Amassing evidence to discern a glacial influence in the deep-time record

Detecting glaciation in Earth's pre-Quaternary record has long relied upon features such as striations that can be rare even in modern systems, and moreover that preserve poorly. This, together with the universal tendency of glaciers to cannibalize their own deposits, and/or be removed by post-glacial erosion aided by isostatic rebound conspires to produce exceedingly patchy evidence for glaciation—even for the case of continental glaciation (e.g., Bjørlykke, 1985). For example, Bell and Laine (1985) estimated that <6% of the glacial sediment produced by the Laurentide ice sheet remains preserved on land. The preservational challenges are multiplied many fold in the case of upland glaciation, given its location in regions typically subject to wholesale erosion, meaning that ice-contact landforms and deposits are subject to complete erasure. The glacial "buzz saw" — rapid glacial denudation above the equilibrium line altitude—places an upper limit on the relief of modern orogens (e.g., Brozovic et al., 1997; Spotila et al., 2004; Mitchell and Montgomery, 2006; Whipple, 2009), and leads to the mobilization and loss of substantial volumes of eroded material from ancient glaciated orogens.

Given this, detecting glaciation in paleo-uplands requires close examination of deposits preserved near the uplands to assess possible proglacial attributes. This paper highlights various attributes of a potential paleo-alpine glacial system; Table 4 synthesizes their relative effectiveness as possible indicators of an upland glacial origin. Distinguishing proglacial from nonglacial alluvial and fluvial facies is non-trivial, as the examples of the Cutler and Fountain systems discussed above illustrate; only recently have these been reinterpreted as proglacial—interpretations which remain controversial. A proglacial interpretation for the Cutler fluvial system benefits from its hypothesized association with an inferred paleovalley (Unaweep Canyon), as well as interpreted ice-contact facies preserved adjacent to the paleo-uplift. Still, in the absence of such preservation of ice-contact attributes, proglacial and periglacial indicators can persist, providing veiled clues to a cold past. Features such as a predominance of HFF, debris flow, and flood (e.g., large-scale cross-beds) strata signaling abundant water and sediment, yet characterized by minimal evidence for chemical weathering suggests cold-wet conditions. Additional evidence for cold temperatures, such as rip-up clasts of non-cohesive material, microtextures indicating glacial grinding, and frozen-ground phenomena would then bolster a proglacial interpretation. Documentation of time-correlative paleo-loess deposits more distally, or loess-derived eolian-marine strata with characteristics consistent with glacial grinding could be preserved up to 100 s to >1000 km from ice margins. Ultimately, building the case for possible upland glaciation requires integration of multiple lines of evidence, none of which might be uniquely diagnostic when considered individually—analogous to building the case for continental glaciation (e.g., see review by Isbell et al., 2021). Although we focus here on upland systems owing to the particularly poor preservation of ice-contact attributes, these same approaches are applicable to detecting glaciation for continental glaciation.

4.2 Implications of assessing upland glaciation in the geologic record

Whether or not the pacing of their advances and retreats harmonizes with those of continental glaciers, alpine glaciers are a sensitive archive of climate change. Their equilibrium line altitudes correlate strongly with regional to global temperature and local precipitation (Clark and Bartlein, 1995; Hastenrath, 2009; Heavens, 2021). The more difficult question to consider is whether they could *drive* regional to global climate change, either by a direct ice-albedo effect or by indirect effects of surface thermophysical properties (including albedo) on cloud dynamics.

In this regard, the major region of alpine glaciation whose effects on climate and climate change have been of interest to climate modelers is the Himalayas and Tibetan Plateau, mountainous regions of high elevation near 30°N. The Tibetan Plateau in particular acts as a winter heat sink and summer heat source to the middle and upper troposphere (Ye, 1981). The Tibetan Plateau thus supports anticyclonic circulation in the upper troposphere in the summer, which coheres well with a strong Indian and Asian summer monsoon (e.g., Hahn and Manabe, 1975; KutzbachPrell and Ruddiman, 1993). The Tibetan Plateau in particular seems necessary to produce this effect, as opposed to just the Himalayas (e.g., Chen et al., 2014). Therefore, Earth historians generally have connected the development of these monsoonal circulations to the uplift of the Tibetan Plateau over the course of the late Cenozoic (e.g., Zhisheng et al., 2001). In the winter, the Tibetan Plateau's strength as a heat sink is proportional to snow cover, resulting in lower geopotential height and a stronger jet stream (e.g., Li et al., 2018). However, spring dust storm activity is dependent on positive spring sensible

heat flux, so lower snow cover should lead to increased west Chinese dust storms (Xie et al., 2020).

Therefore, we would hypothesize that lowered ELA and more widespread Tibetan Plateau glaciation would tend to transform the Tibetan Plateau into a year-round heat sink, suppressing the monsoonal circulations around it and favoring year-round cyclonic circulation aloft. Indeed, the Indian monsoon precipitation was much lower than present at the Last Glacial Maximum (e.g., Jalihal et al., 2019), but any role for the Tibetan Plateau may have been swamped by continental ice sheet and greenhouse gas effects (Cao et al., 2019). It is also possible that the Tibetan Plateau did not significantly glaciate at the Last Glacial Maximum (Liu et al., 2020). Rather, there was merely an advance in permafrost.

That said, the general dynamical role of being a mid-upper troposphere heat source or sink may hold more generally for sufficiently high alpine areas. At the Equator, the seasonality of these effects will decrease greatly. For an unglaciated mountain range, such a mountain range will be a year-round heat source. However, as glaciation increased, it could be expected to become at some point, a heat sink.

A practical example of such a range would be the Appalachian and Hercynian orogenic belts, which formed an extremely long mountain range spanning >5000 km near the Equator (e.g., Kent and Muttoni, 2020), the Central Pangaean Mountains (CPM). Such a range would tend to focus peak heating at the Equator if weakly glaciated and displace peak heating from the Equator if strongly glaciated. The role of orography and other zonal asymmetries in Hadley cell and monsoonal dynamics remains hotly debated (e.g., Geen et al., 2020). Theoretical arguments extended by Lindzen and Hou (1988) would suggest that displacement of peak heating off the Equator would generate a strongly asymmetric circulation with a strong winter Hadley cell and a negligible summer Hadley cell. This forcing acting over a significant, but still small fraction of the planetary circumference could be presumed to lead to a strong summer monsoon or monsoon-like circulation, perhaps explaining the pseudo-monsoonal circulation around the CPM produced by a glaciated CPM in a climate model simulation (Heavens et al., 2015).

A similar argument could be made on the basis of idealized simulations that consider the response of the circulation to an isolated heat source. The initial response is a region of westerly flow at the Equator with cyclonic circulation in the tropics to the north and south (i.e., Pangaea) (Matsuno, 1966; Gill, 1980; Wu et al., 2001; Vallis and Penn, 2020), again a pseudo-monsoonal circulation in that it reverses the normal wind direction at the Equator, though persistently rather than seasonally. The extent of these circulations is a function of damping (presumably mostly radiative in the real atmosphere). This disturbance then can propagate eastward as a convective complex, drawing cold, dry air behind it and enhancing evaporation ahead of it. The consequence is to focus convective activity and rainfall to the east of the heat source.

Reasoning from Gill (1980), an isolated heat sink should cause the exactly reverse scenario, with a positive easterly wind anomaly and anticyclonic flow in the northern and southern Pangaean tropics. This situation would reduce precipitation by two mechanisms: dry continental subtropical air would expand over the tropics, while convection at the Equator would be suppressed by the strong inversion at the frozen surface. Some enhancement of precipitation in the western Panthalassic ocean would be possible. Heavens et al. (2015)'s glaciated CPM simulation does suggest a negative Gill-type response, with significantly reduced precipitation in equatorial and eastern tropical Pangaea (in the cooling zone and to its northeast and southeast, where anticyclonic flow would result in winds coming from the subtropics); non-anomalous precipitation in western tropical Pangaea and increased precipitation in western subtropical Pangaea (to the northwest and southwest of the cooling zone, where anticyclonic flow would come from the Equator).

The net consequence seems to be much greater aridity over equatorial and eastern tropical Pangaea. If this occurred episodically with changes in orbital forcing/ice sheet expansion, it would greatly enhance the effects of those changes on tropical climate. Uplift coinciding with low equilibrium line altitudes in the cold global climates of the late Carboniferous could explain the greater sensitivity of Euramerican coal forests to glacial-interglacial changes near the Moscovian-Kasimovian boundary and the coal forest breakdown that followed (Falcon-Lang and DiMichele, 2010). However, more detailed modeling of this scenario would be necessary to understand its consequences, because Heavens et al. (2015) also expands continental ice sheets in addition to glaciating the CPM.

The final question to ask is whether alpine glaciation might enable an ice-albedo feedback like that of continental ice sheets, that is, with substantive impact on global temperature. The CPM is the best candidate for having such an effect on account of its size and its equatorial location. If it were glaciated to 2000 m elevation, the glaciated CPM alone reasonably could have an area of up to 1% of the Earth's surface (~3.3% of the Earth's surface is above 2000 m elevation today). Ignoring cloud albedo changes, its albedo would change from ~0.3 to ~0.9. Assuming 97.5% of present day insolation (Heavens et al., 2015), glaciation of the CPM to 2000 m from minimal glaciation would result in a negative radiative forcing of ~4 Wm^{-2}, a similar magnitude—albeit opposite sign—as a doubling in pCO_2 (3.7 Wm^{-2}) (Myrhe et al., 2017). Depending on the total sensitivity of the Earth system (e.g., Wong et al., 2021), CPM glaciation could be expected to result in a further decrease in global temperature by 2.8°C–5°C, perhaps enhancing the amplitude of glacial-interglacial temperature variability significantly. Note that widespread glaciation of the CPM and its effects on regional climate could be self-limiting. Reduced precipitation could raise ELA (Mote and Kaser, 2007; Heavens, 2021). If precipitation is low, glaciers can ablate by direct sunlight well above the level where mean air temperatures are below

freezing, because there is not enough snowfall to replenish lost meltwater formed during the day.

5 Conclusion

Continental glaciers leave distinctive marks in the geologic record, in the form of both glaciated surfaces and ice-contact deposits subject to potential preservation owing to their deposition in low-elevation regions commonly below baselevel. In contrast, the geologic record of upland glaciation is particularly meager, with extremely low preservation potential. Yet, far from being insignificant, glaciation in uplands responds to and can even influence the global climate system. Capturing the extent of glaciation in upland regions is therefore critical to accurate hindcasts of Earth's climate states. Furthermore, even reconstructions of continental ice sheets can—and do—suffer from the pervasive cannibalistic character of glaciation, wherein deposits are eroded by subsequent ice advances and ablation, and by the effects of isostatic rebound, causing difficulty in accurate reconstructions of the extents of former glaciations. Stratigraphic records of pro- and peri-glacial deposits, and attention to identification of loessite and silt-rich epeiric sea strata that can signal the operation of glacial grinding can help refine reconstructions of the extent of glaciation in Earth's deep-time past.

Ethics Statement

Written informed consent was obtained from the individual(s) for the publication of any identifiable images or data included in this article.

Author Contributions

GS conceived and drafted the manuscript and, together with LP collated data for the loess review; LP focused on the case study of the Salagou Formation; DS focused on the microtextural and proglacial sections, with contributions from GS and LP, NH wrote on implications for climate modeling, and all authors contributed to writing and revising the manuscript and preparing figures. All authors approved the submitted version.

Funding

Work summarized in this paper was completed with funding from the U.S. National Science Foundation under the following grant numbers: EAR-9805130, 0001052, 0230332, 0746042, 1053018, 1338331, OISE-1658614 to GSS, EAR-1324818 to DES, and EAR-1849754 to NGH.

Acknowledgments

We thank the US National Science Foundation (grant numbers cited above) for financial support of our work. Thank you to editors John Isbell and Fernando Vesely, and to Christopher Fielding and György Varga, for constructive critiques of the manuscript. Thanks to M. J. Soreghan and to many University of Oklahoma students who have contributed to various aspects of this work over the years, and to our collaborators S. Pochat and J. Van Den Driessche for help with our work on the French Permian. We respectfully acknowledge the longstanding significance of lands studied herein for Indigenous Peoples past, present, and future.

Conflict of interest

The authors declare that the research was conducted in the absence of any commercial or financial relationships that could be construed as a potential conflict of interest.

Publisher's note

References

Adams, S. M., and Soreghan, G. S. (2020). A test of the efficacy of sand saltation for silt production: Implications for the interpretation of loess. *Geology* 48 (11), 1105–1109. doi:10.1130/G47282.1

Alexander, J., Bridge, J. S., Cheel, R. J., and Leclair, S. F. (2001). Bedforms and associated sedimentary structures formed under supercritical water flows over aggrading sand beds. *Sedimentology* 48 (1), 133–152. doi:10.1046/j.1365-3091.2001.00357.x

Allan, J. A. (1926). Ice crystal markings. *Am. J. Sci.* 5 (11), 494–500. doi:10.2475/ajs.s5-11.66.494

Anderson, R. C. (1955). Pebble lithology of the Marseilles till sheet in northeastern Illinois. *J. Geol.* 63, 228–243. doi:10.1086/626252

Aquino, C. D., Milana, J. P., and Faccini, U. F. (2014). New glacial evidences at the Talacasto paleofjord (Paganzo basin, W-Argentina) and its implications for the paleogeography of the Gondwana margin. *J. S. Am. Earth Sci.* 56, 278–300. doi:10.1016/j.jsames.2014.09.001

Assallay, A. M., Rogers, C. D. F., Smalley, I. J., and Jefferson, I. F. (1998). Silt: 2–62 μm, 9–4φ. *Earth-Science Rev.* 45, 61–88. doi:10.1016/s0012-8252(98)00035-x

Atkins, C. B. (2003). *Characteristics of striae and clast shape in glacial and non-glacial environments*. Dissertation. Wellington, New Zealand: Victoria University of Wellington.

Atkins, C. B. (2004). Photographic atlas of striations from selected glacial and non-glacial environments. *Antarct. Data Ser.* 28 (45). ISSN: 0375-8192.

Baars, D. L. (1962). Permian system of Colorado plateau. *Am. Assoc. Petroleum Geol. Bull.* 46, 149–218. doi:10.1306/BC74376F-16BE-11D7-8645000102C1865D

Baas, J. H., Best, J. L., and Peakall, J. (2011). Depositional processes, bedform development and hybrid bed formation in rapidly decelerated cohesive (mud–sand) sediment flows. *Sedimentology* 58 (7), 1953–1987. doi:10.1111/j.1365-3091.2011.01247.x

Baas, J. H., Best, J. L., and Peakall, J. (2016). Predicting bedforms and primary current stratification in cohesive mixtures of mud and sand. *J. Geol. Soc.* 173 (1), 12–45. doi:10.1144/jgs2015-024

Ballance, P. F. (1984). Sheet-flow-dominated gravel fans of the non-marine Middle Cenozoic Simmler Formation, Central California. *Sediment. Geol.* 38, 337–359. doi:10.1016/0037-0738(84)90085-x

Batalla, R. J., De Jong, C., Ergenzinger, P., and Sala, M. (1999). Field observations on hyperconcentrated flows in mountain torrents. *Earth Surf. Process. Landforms J. Br. Geomorphol. Res. Group* 24 (3), 247–253. doi:10.1002/(sici)1096-9837(199903)24:3<247::aid-esp961>3.0.co;2-1

Begam, S., Sen, D., and Dey, S. (2018). Moraine dam breach and glacial lake outburst flood generation by physical and numerical models. *J. Hydrology* 563, 694–710. doi:10.1016/j.jhydrol.2018.06.038

Bell, M., and Laine, E. P. (1985). Erosion of the Laurentide region of North America by glacial and glaciofluvial processes. *Quat. Res.* 23, 154–174. doi:10.1016/0033-5894(85)90026-2

Benn, D., and Evans, D. J. (2010). *Glaciers and glaciation*. New York, NY: Routledge, 802.

Benvenutti, M., and Martini, I. P. (2002). "Analysis of terrestrial hyperconcentrated flows and their deposits,". *Flood and megaflood processes and deposits: Recent and ancient examples*. Editors I. P. Martini, V. R. Baker, and G. Garzón (Ghent, Belgium: International Association of Sedimentologists, Special Publication), 32, 167–193.

Berti, M., Genevois, R., Simmoni, A., and Tecca, P. R. (1999). Field observations of a debris flow event in the Dolomites. *Geomorphology* 29, 265–274. doi:10.1016/s0169-555x(99)00018-5

Best, J. L. (1992). Sedimentology and vent timing of a catastrophic volcaniclastic mass flow, Volcan Hudson, Southern Chile. *Bull. Volcanol.* 54, 299–318. doi:10.1007/bf00301484

Beverage, J. P., and Culbertson, J. H. (1964). Hyperconcentrations of suspended sediment. American society of civil engineers proceedings. *J. Hydraulics Div.* 90, 117–126. doi:10.1061/jyceaj.0001128

Bjørlykke, K. (1985). Glaciations, preservation of the sedimentary record and sea level changes — A discussion based on the late precambrian and lower palaeozoic sequences in Norway. *Palaeogeogr. Palaeoclimatol. Palaeoecol.* 51, 197–207. doi:10.1016/0031-0182(85)90085-9

Black, R. F. (1976). Periglacial features indicative of permafrost: Ice and soil wedges. *Quat. Res.* 6, 3–26. doi:10.1016/0033-5894(76)90037-5

Blažauskas, N., Jurgaitis, A., and Šinkūnas, P. (2007). Patterns of late Pleistocene proglacial fluvial sedimentation in the SE Lithuanian plain. *Sediment. Geol.* 193 (1-4), 193–201. doi:10.1016/j.sedgeo.2005.06.015

Boothroyd, J. C., and Ashley, G. M. (1975). "Process, bar morphology, and sedimentary structures on braided outwash fans, northeastern Gulf of Alasks,". *Glacio-fluvial and glaciolacustrine sedimentation*. Editors A. V. Jopling and B. C. McDonald (Tulsa, Oklahoma: Society of Economic Paleontologists and Mineralogists Special Paper), 23, 193–222. doi:10.2110/pec.75.23.0193

Boothroyd, J. C., and Nummendal, D. (1978). "Proglacial braided outwash: A model for humid alluvial-fan deposits,". *Fluvial sedimentology: Canadian society of petroleum geologists memoir*. Editor A. D. Miall, 5, 641–668.

Boulton, G. S. (1979). Processes of glacier erosion on different substrata. *J. Glaciol.* 23, 15–38. doi:10.3189/s0022143000029713

Breien, H., De Blasio, F. V., Elverhoi, A., and Hoeg, K. (2008). Erosion and morphology of a debris flow caused by a glacial lake outburst flood, Western Norway. *Landslides* 5, 271–280. doi:10.1007/s10346-008-0118-3

Brennand, T. A., and Shaw, J. (1996). The harricana glacifluvial complex, abitibi region, quebec: Its Genesis and implications for meltwater regime and ice-sheet dynamics. *Sediment. Geol.* 102, 221–262. doi:10.1016/0037-0738(95)00069-0

Bridge, J., and Demicco, R. (2008). Earth surface processes, landforms and sediment deposits. *Earth Surf. Process.*, 815. 516 doi:10.1017/cbo9780511805516

Bristow, C. S., Drake, N., and Armitage, S. (2009). Deflation in the dustiest place on Earth: The Bodele depression, Chad. *Geomorphology* 105, 50–58. doi:10.1016/j.geomorph.2007.12.014

Brown, J. E. (1973). Depositional histories of sand grains from surface textures. *Nature* 242, 396–398. doi:10.1038/242396a0

Browzin, B. S. (1985). Granular loess classification based on loessial fraction. *Bull. Assoc. Eng. Geol.* XXII (2), 217–227. doi:10.2113/gseegeosci.xxii.2.217

Brozovic, N., Burbank, D. W., and Meigs, A. J. (1997). Climatic limits on landscape development in the northwestern Himalaya. *Science* 276, 571–574. doi:10.1126/science.276.5312.571

Bull, W. B. (1963). Alluvial-fan deposits in western fresno county, California. *J. Geol.* 71, 243–251. doi:10.1086/626896

Bullard, J. E., McTainsh, G. H., and Pudmenzky, C. (2004). Aeolian abrasion and modes of fine particle production from natural red dune sands: An experimental study. *Sedimentology* 51, 1103–1125. doi:10.1111/j.1365-3091.2004.00662.x

Bullard, J. E., McTainsh, G. H., and Pudmenzky, C. (2007). Factors affecting the nature and rate of dust production from natural dune sands. *Sedimentology* 54, 169–182. doi:10.1111/j.1365-3091.2006.00827.x

Calhoun, N. C., and Clague, J. J. (2018). Distinguishing between debris flows and hyperconcentrated flows: An example from the eastern Swiss Alps. *Earth Surf. Process. Landforms* 43 (6), 1280–1294. doi:10.1002/esp.4313

Campbell, J. A. (1979). "Lower Permian depositional system, northern Uncompahgre basin," in *Permian land field symposium*. Editor D. L. Baars (Four Corners Geological Society Guidebook), 13–21.9. Available at: https://archives.datapages.com/data/fcgs/data/015/015001/13_four-corners150013.htm.

Campbell, J. A. (1980). "Lower Permian depositional systems and Wolfcampian paleogeography, Uncompahgre basin, eastern Utah and southwestern Colorado," in *Paleozoic paleogeography of west-central United States, SEPM, rocky mountain section*. Editors T. D. Fouch and E. R. Magathan, 327–340.

Cao, W., Flament, N., Zahirovic, S., Williams, S., and Müller, R. D. (2019). The interplay of dynamic topography and eustasy on continental flooding in the late Paleozoic. *Tectonophys.* 761, 108–121. doi:10.1016/j.tecto.2019.04.018

Carvajal, C. P., Soreghan, G. S., Isaacson, P. E., Ma, C., Hamilton, M. A., Hinnov, L. A., et al. (2018). Atmospheric dust from the Pennsylvanian Copacabana Formation (Bolivia): A high-resolution record of paleoclimate and volcanism from northwestern Gondwana. *Gondwana Res.* 58, 105–121. doi:10.1016/j.gr.2018.02.007

Cater, F. W., Jr. (1970). Geology of the salt anticline region in southwestern Colorado: U.S. Geological survey, Professional Paper 637, 80.

Catt, J. A. (1988). "Loess—its formation, transport and economic significance," in *Physical and chemical weathering in geochemical cycles. NATO ASI series (series C: Mathematical and physical Sciences)*. Editors A. Lerman and M. Meybeck (Dordrecht: Springer), 251. doi:10.1007/978-94-009-3071-1_6

Chan, M. A. (1999). Triassic loessite of north-central Utah: Stratigraphy, petrophysical character, and paleoclimate implications. *J. Sediment. Res.* 69, 477–485. doi:10.2110/jsr.69.477

Chen, G.-S., Liu, Z., and Kutzbach, J. E. (2014). Reexamining the barrier effect of the Tibetan Plateau on the South Asian summer monsoon. *Clim. Past.* 10, 1269–1275. doi:10.5194/cp-10-1269-2014

Chen, J., Liu, X., and Liu, X. (2019). Sedimentary dynamics and climatic implications of Cretaceous loess-like red beds in the Lanzhou basin, Northwest China. *J. Asian Earth Sci.* 180, 103865. doi:10.1016/j.jseaes.2019.05.010

Clark, P. U., and Bartlein, P. J. (1995). Correlation of late Pleistocene glaciation in the wester United States with north atlantic heinrich events. *Geology* 23 (6), 483–486. doi:10.1130/0091-7613(1995)023<0483:colpgi>2.3.co;2

Clarke, J. M. (1918). "Strand and undertow markings of upper devonian time as indications of the prevailing climate," in *New York State museum bulletin*, 199–210.

Costa, P. J., Park, Y. S., Kim, Y. D., Quintela, M., Mahaney, W. C., Dourado, F., et al. (2017). Imprints in silica grains induced during an open-channel flow experiment: Determination of microtextural signatures during aqueous transport. *J. Sediment. Res.* 87 (7), 677–687. doi:10.2110/jsr.2017.39

Crouvi, O., Amit, R., Enzel, Y., Porat, N., and Sandler, A. (2008). Sand dunes as a major proximal dust source for late Pleistocene loess in the Negev desert, Israel. *Quat. Res.* 70 (2), 275–282. doi:10.1016/j.yqres.2008.04.011

Crowell, J. C. (1978). Gondwanan glaciation, cyclothems, continental positioning, and climate change. *Am. J. Sci.* 278, 1345–1372. doi:10.2475/ajs.278.10.1345

Crowell, J. C. (1999). Pre-Mesozoic ice ages: Their bearing on understanding the climate system. *Geol. Soc. Am. Mem.* 192, 122. doi:10.1130/MEM192

Cui, P., Dang, C., Cheng, Z., and Scott, K. M. (2010). Debris flows resulting from glacial-lake outburst floods in Tibet, China. *Phys. Geogr.* 31 (6), 508–527. doi:10.2747/0272-3646.31.6.508

Davies, T. R., Smart, C. C., and Turnbull, J. M. (2003). Water and sediment outbursts from advanced Franz Josef glacier, New Zealand. *Earth Surf. Process. Landforms J. Br. Geomorphol. Res. Group* 28 (10), 1081–1096. doi:10.1002/esp.515

De Blasio, F. V., Breien, H., and Elverhøi, A. (2011). Modelling a cohesive-frictional debris flow: An experimental, theoretical, and field-based study. *Earth Surf. Process. Landforms* 36 (6), 753–766. doi:10.1002/esp.2101

de Haas, T., McArdell, B. W., Nijland, W., Åberg, A. S., Hirschberg, J., and Huguenin, P. (2022). Flow and bed conditions jointly control debris-flow erosion and bulking. *Geophys. Res. Lett.* 49, e2021GL097611. doi:10.1029/2021gl097611

Dessouki, T. C. E. (2009). *Water quality assessment of the salmon river near hyder, Alaska 1990-2007*. British Columbia, Canada: British Columbia Ministry of Environment Report, 23.

Dingle, E. H., Kusack, K. M., and Venditti, J. G. (2021). The gravel-sand transition and grain size gap in riverbed sediments. *Earth-Science Rev.* 222, 103838. doi:10.1016/j.earscirev.2021.103838

Dubois, M. K., Goldstein, R. H., and Hasiotis, S. T. (2012). Climate-controlled aggradation and cyclicity of continental loessic siliciclastic sediments in Asselian-Sakmarian cyclothems, Permian, Hugoton Embayment, USA. *Sedimentology* 59 (6), 1782–1816. doi:10.1111/j.1365-3091.2012.01326.x

Dykstra, M., Kneller, B., and Milana, J. P. (2006). Deglacial and postglacial sedimentary architecture in a deeply incised paleovalley-paleofjord—The Pennsylvanian (late Carboniferous) Jejenes Formation, San Juan, Argentina. *GSA Bullet.* 118 (7-8), 913–937. doi:10.1130/B25810.1

Edwards, M. B. (1979). Late Precambrian glacial loessites from north Norway and Svalbard. *J. Sediment. Petrology* 49, 85–92. doi:10.1306/212F76C6-2B24-11D7-8648000102C1865D

Elston, D. P., and Shoemaker, E. M. (1960). "Late paleozoic and early mesozoic structural history of the Uncompahgre front," in *Geology of the Paradox basin fold and fault belt: Four corners geological society, third field conference*. Editors K. G. Smith, D. Kirkland, and R. Byington, 47–55.

Enzel, Y., Amit, R., Crouvi, O., and Porat, N. (2010). Abrasion-derived sediments under intensified winds at the latest Pleistocene leading edge of the advancing Sinai-Negev erg. *Quat. Res.* 74, 121–131. doi:10.1016/j.yqres.2010.04.002

Falcon-Lang, H. J., and DiMichele, W. A. (2010). What happened to the coal forests during glacial phases? *Palaios* 25, 611–617. doi:10.2110/palo.2009.p09-162r

Fellows, R. H., Jr. (1951). *Experiments in the formation of desiccation cracks sediments*. MS Thesis. Dallas, Texas: Southern Methodist University.

Fenton, C. R., Webb, R. H., and Cerling, T. E. (2006). Peak discharge of a Pleistocene lava-dam outburst flood in Grand Canyon, Arizona, USA. *Quat. Res.* 65 (02), 324–335. doi:10.1016/j.yqres.2005.09.006

Fielding, C. R., Sliwa, R., Holcombe, R. J., and Kassan, J. (2000). "January. A new palaeogeographic synthesis of the Bowen Basin of central Queensland," in *Bowen basin symposium 2000 proceedings*. Editors J. Beeston (Rockhampton: Geological Society of Australia Coal Geology Group), 287–302.

Fielding, C. R. (2006). Upper flow regime sheets, lenses and scour fills: Extending the range of architectural elements for fluvial sediment bodies. *Sediment. Geol.* 190 (1-4), 227–240. doi:10.1016/j.sedgeo.2006.05.009

Fisher, R. V. (1983). Flow transformation in sediment gravity flows. *Geology* 11, 273–274. doi:10.1130/0091-7613(1983)11<273:ftisgf>2.0.co;2

Foster, T. M., Soreghan, G. S., Soreghan, M. J., Benison, K. C., and Elmore, R. D. (2014). Climatic and paleogeographic significance of eolian sediment in the middle permian Dog Creek shale (midcontinent U.S.). *Palaeogeogr. Palaeoclimatol. Palaeoecol.* 402, 12–29. doi:10.1016/j.palaeo.2014.02.031

French, H. M. (2013). *The periglacial environment*. John Wiley & Sons, 478.

French, H., and Shur, Y. (2010). The principles of cryostratigraphy. *Earth-Science Rev.* 101 (3–4), 190–206. doi:10.1016/j.earscirev.2010.04.002

Geen, R., Bordoni, S., Battisti, D. S., and Hui, K. (2020). Monsoons, ITCZs, and the concept of the global monsoon. *Rev. Geophys.* 58, 700. doi:10.1029/2020RG000700

Giles, J. M., Soreghan, M. J., Benison, K. C., Soreghan, G. S., and Hasiotis, S. T. (2013). Lakes, loess, and paleosols in the Permian Wellington Formation of Oklahoma, U.S.A: Implications for Paleoclimate and Paleogeography of the Midcontinent. *J. Sediment. Res.* 83, 825–846. doi:10.2110/jsr.2013.59

Gill, A. E. (1980). Some simple solutions for heat-induced tropical circulation. *Q. J. R. Meteorol. Soc.* 106, 447–462. doi:10.1002/qj.49710644905

Girard, F., Ghienne, J., Du-bernard, X., and Rubino, J. (2015). Sedimentary imprints of former ice-sheet margins: Insights from an end-Ordovician archive (SW Libya). *Earth Sci. Rev.* 148, 259–289. doi:10.1016/j.earscirev.2015.06.006

Haberlah, D., Williams, M. A. J., Halverson, G., McTainsh, G. H., Hill, SlM., Hrstka, T., et al. (2010). Loess and floods: High-resolution multi-proxy data of (LGM) slackwater deposition in the Flinders Ranges, semi-arid South Australia Last Glacial Maximum. *Quat. Sci. Rev.* 29, 2673–2693. doi:10.1016/j.quascirev.2010.04.014

Hahn, D. G., and Manabe, S. (1975). The Role of Mountains in the South Asian Monsoon Circulation. *J. Atmos. Sci.* 32 (8), 1515–1541. doi:10.1175/1520-0469(1975)032<1515:tromit>2.0.co;2

Hambrey, M. J. (1994). *Glacial environments*. Vancouver, British Columbia: UBC Press, University of British Columbia, 296.

Hampton, M. A. (1972). The role of subaqueous debris flow in generating turbidity currents. *J. Sediment. Petrology* 42, 775–793. doi:10.1306/74d7262b-2b21-11d7-8648000102c1865d

Hampton, M. A. (1975). Competence of fine-grained debris flows. *J. Sediment. Petrology* 45, 834–844. doi:10.1306/212F6E5B-2B24-11D7-8648000102C1865D

Hampton, M. A. (1979). Buoyancy in debris flows. *J. Sediment. Petrology* 49, 0753–0758. doi:10.1306/212F7838-2B24-11D7-8648000102C1865D

Harrison, S., and Fritz, W. J. (1982). Depositional features of March 1982 Mount St. Helens sediment flows. *Nature* 299, 720–722. doi:10.1038/299720a0

Hart, J. K. (2006). An investigation of subglacial processes at the microscale from Briksdalsbreen, Norway. *Sedimentology* 53 (1), 125–146. doi:10.1111/j.1365-3091.2005.00758.x

Hastenrath, S. (2009). Past glaciation in the tropics. *Quat. Sci. Rev.* 28 (9), 790–798. doi:10.1016/j.quascirev.2008.12.004

Heavens, N. G. (2021). Downscaling CESM2 in CLM5 to hindcast preindustrial equilibrium line altitudes for tropical mountain glaciers. *Geophys. Res. Lett.* 48, e2021GL094071. doi:10.1029/2021GL094071

Heavens, N. G., Mahowald, N. M., Soreghan, G. S., Soreghan, M. J., and Shields, C. A. (2015). A model-based evaluation of tropical climate in Pangaea during the late Palaeozoic Icehouse. *Palaeogeogr. Palaeoclimatol. Palaeoecol.* 425, 109–127. doi:10.1016/j.palaeo.2015.02.024

Henry, L. C., Isbell, J. L., Limarino, C. O., Mchenry, L. J., and Fraiser, M. L. (2010). Mid-Carboniferous deglaciation of the Protoprecordillera, Argentina recorded in the Agua de Jagüel Palaeovalley. *Palaeogeogr. Palaeoclimatol. Palaeoecol.* 298 (1–2), 112–129. doi:10.1016/j.palaeo.2010.03.051

Hungr, O., and McDougall, S. (2005). "Bovis M.Entrainment of material by debris flows," in *Debris-flow hazards and related phenomena*. Editors M. Jakob and O. Hungr (Berlin: Springer), 135–158.

Isbell, J. L., Miller, M. F., Wolfe, K. L., and Lenaker, P. A. (2003). "Timing of late Paleozoic glaciation in Gondwana: Was glaciation responsible for the development of northern hemisphere cyclothems?," in *Extreme depositional environments: Mega end members in geologic time: Boulder, Colorado*. Editors M. A. Chan and A. W. Archer (Boulder, CO: Geological Society of America Inc.), 5–24. doi:10.1130/0-8137-2370-1.5

Isbell, J. L., Henry, L. C., Gulbranson, E. L., Limarino, C. O., Fraiser, M. L., Kock, Z. J., et al. (2012). Glacial paradoxes during the late Paleozoic ice age: Evaluating the equilibrium line altitude as a control on glaciation. *Gondwana Res.* 22, 1–19. doi:10.1016/j.gr.2011.11.005

Isbell, J. L., Vesely, F. L., Rosa, E. L. M., Pauls, K. N., Fedorchuk, N. D., Ives, L. R. W., et al. (2021). Evaluation of physical and chemical proxies used to interpret past glaciations with a focus on the Late Paleozoic Ice Age. *Earth-Science Rev.* 221, 756. doi:10.1016/j.earscirev.2021.103756

Jalihal, C., Srinivasan, J., and Chakraborty, A. (2019). Modulation of Indian monsoon by water vapor and cloud feedback over the past 22,000 years. *Nat. Commun.* 10, 5701. doi:10.1038/s41467-019-13754-6

Jefferson, I., Rosenbaum, M., and Smalley, I. (2002). Mercia Mudstone as a Triassic aeolian desert sediment. *Mercian Geol.* 15, 157–162.

Johnson, S. Y. (1989). Significance of loessite in the Maroon Formation (Middle Pennsylvanian to Lower Permian), Eagle Basin, northwestern Colorado. *J. Sediment. Petrology* 59, 782–791. doi:10.1306/212F9070-2B24-11D7-8648000102C1865D

Jones, A. T., and Fielding, C. R. (2008). Sedimentary facies of a glacially influenced continental succession in the Pennsylvanian Jericho Formation, Galilee Basin, Australia. *Sedimentol.* 55, 531–556. doi:10.1111/j.1365-3091.2007.00911.x

Kalińska, E., Lamsters, K., Karušs, J., Krievāns, M., Rečs, A., and Ješkins, J. (2021). Does glacial environment produce glacial mineral grains? Pro-and supra-glacial Icelandic sediments in microtextural study. *Quat. Int.* 617, 101–111. doi:10.1016/j.quaint.2021.03.029

Kalińska-Nartiša, E., and Gałka, M. (2018). Sand in Early Holocene lake sediments–a microscopic study from Lake Jaczno, northeastern Poland. *Est. J. Earth Sci.* 67 (2), 122–132. doi:10.3176/earth.2018.09

Kalińska-Nartiša, E., Woronko, B., and Ning, W. (2017). Microtextural inheritance on quartz sand grains from Pleistocene periglacial environments of the Mazovian Lowland, central Poland. *Permafr. Periglac. Process.* 28 (4), 741–756. doi:10.1002/ppp.1943

Kalińska-Nartiša, E., Stivrins, N., and Grudzinska, I. (2018). Quartz grains reveal sedimentary palaeoenvironment and past storm events: A case study from eastern Baltic. Estuarine. *Coast. Shelf Sci.* 200, 359–370. doi:10.1016/j.ecss.2017.11.027

Kaser, G. (2009). "Mountain Glaciers," in *Glacier science and environmental change*. Editor P. G. Knight (Oxford, UK: Wiley-Blackwell), 268–271.

Kataoka, K. S., Urabe, A., Manville, V., and Kajiyama, A. (2008). Breakout flood from an ignimbrite-dammed valley after the 5 ka Numazawako eruption, northeast Japan. *Geol. Soc. Am. Bull.* 120 (9-10), 1233–1247. doi:10.1130/b26159.1

Keiser, L. J., Soreghan, G. S., and Kowalewski, M. (2015). Use of quartz microtextural analysis to assess possible proglacial deposition for the Pennsylvanian-Permian Cutler Formation (Colorado, U.S.A.). *J. Sediment. Res.* 85, 1310–1322. doi:10.2110/jsr.2015.81

Kenis, P., Skurzynski, J., Zdzisław, J., and Kubik, R. (2020). A new methodological approach (QEMSCAN) in the mineralogical study of Polish loess: Guidelines for further research. *Open Geosci.* 12, 1. doi:10.1515/geo-2020-0138

Kent, D. V., and Muttoni, G. (2020). Pangea B and the Late Paleozoic Ice Age. *Palaeogeogr. Palaeoclimatol. Palaeoecol.* 553, 1. doi:10.1016/j.palaeo.2020.109753

Kessler, J. L. P., Soreghan, G. S., and Wacker, H. J. (2001). Depositional and pedogenic evidence for equatorial aridity in Western Pangea: Upper Paleozoic loessite of northeastern New Mexico. *J. Sediment. Res.* 71, 818–833. doi:10.1306/2dc4096b-0e47-11d7-8643000102c1865d

Kirshner, A. E., and Anderson, J. B. (2011). "Cenozoic glacial history of the northern Antarctic Peninsula: A micromorphological investigation of quartz sand grains," in *Tectonic, climatic, and cryospheric evolution of the Antarctic peninsula special publication 63* (American Geophysical Union), 153–165.

Kleppe, J. H., and Olsen, R. E. (1985). *Desiccation cracking of soil barriers: Hydraulic barriers in soil and rock*. American Society for Testing and Materials International.

Kneller, B., Milana, J. P., Buckee, C., and Al Ja'aidi, O. S. (2004). A depositional record of deglaciation in a paleofjord (Late Carboniferous [Pennsylvanian] of San Juan Province, Argentina): The role of catastrophic sedimentation. *Geol. Soc. Am. Bull.* 116, 348–367. doi:10.1130/B25242.1

Krinsley, D. H., and Doornkamp, J. C. (1973). *Atlas of sand grain surface textures*. Cambridge, U.K.: Cambridge University Press, 91.

Krizek, M., Krbcova, K., Mida, P., and Hanacek, M. (2017). Micromorphological changes as an indicator of the transition from glacial to glaciofluvial quartz grains: Evidence from Svalbard. *Sediment. Geol.* 358, 35–43. doi:10.1016/j.sedgeo.2017.06.010

Krzyszkowski, D. (2002). Sedimentary successions in ice-marginal fans of the Late Saalian glaciation, southwestern Poland. *Sediment. Geol.* 149 (1-3), 93–109. doi:10.1016/s0037-0738(01)00246-9

Kuenen, P. H. (1960). Experimental abrasion 4: Eolian action. *J. Geol.* 68, 427–449. doi:10.1086/626675

Kuhn, G., Melles, M., Ehrmann, W. U., Hambrey, M. J., and Schmiedl, G. (1993). Character of clasts in glaciomarine sediments as an indicator of transport and depositional processes, Weddell and Lazarez Seas, Antarctica. *J. Sed. Petrol.* 63, 477–487. doi:10.1306/D4267B2C-2B26-11D7-8648000102C1865D

Kutzbach, J. E., Prell, W. F., and Ruddiman, W. F. (1993). Sensitivity of Eurasian Climate to Surface Uplift of the Tibetan Plateau. *J. Geol.* 101 (2), 177–190. doi:10.1086/648215

Lachenbruch, A. H. (1962). *Mechanics of thermal contraction cracks and ice-wedge polygons in permafrost*, 7. New York, NY: Geological Society of America Inc., 69.

Lang, P. J., Dijon, M., Yahaya, M., El Hamet, M. O., and Besombes, J. C. M. (1991). Depots glaciaires du Carbonifere inferieur a l'Ouest de l'Air (Niger). *Geol. Rundsch.* 80 (3), 611–622. doi:10.1007/bf01803689

Lang, W. B. (1937). The Permian Formations of the Pecos Valley of New Mexico and Texas. *Bull. Am. Assoc. Petroleum Geol.* 21 (7), 833–898. doi:10.1306/3D932EDE-16B1-11D7-8645000102C1865D

Lawson, D. E. (1982). Mobilization, movement and deposition of active subaerial sediment flows, Matanuska Glacier, Alaska. *J. Geol.* 90 (3), 279–300. doi:10.1086/628680

Lawton, T. F., Ruiz Urueña, J. E., Solari, J. A., Terrazas, C. T., Juárez-Arriaga, E., and Ortega-Obregón, C. (2018). "Provenance of Upper Triassic-Middle Jurassic strata of the Plomosas uplift, east-central Chihuahua, Mexico, and possible sedimentologic connections with Colorado Plateau depositional systems," in *Tectonics, sedimentary basins, and provenance: A celebration of william R. Dickinson's career*. Editors R. V. Ingersoll, T. F. Lawton, and S. A. Graham (Boulder, CO: Geological Society of America Inc.), 540, 481–507. doi:10.1130/2018.2540(22)

Li, W., Guo, W., and Qiu, B. (2018). Influence of Tibetan Plateau snow cover on East Asian atmospheric circulation at medium-range time scales. *Nat. Commun.* 9, 4243. doi:10.1038/s41467-018-06762-5

Li, Y., Shi, W., Aydin, A., Beroya-Eitner, M. A., and Gao, G. (2020). Loess Genesis and worldwide distribution. *Earth-Science Rev.* 201, 102947. doi:10.1016/j.earscirev.2019.102947

Li, Z., Yu, X., Dong, S., Chen, Q., and Zhang, C. (2020). Microtextural features on quartz grains from eolian sands in a subaqueous sedimentary environment: A case study in the hinterland of the Badain Jaran Desert, Northwest China. *Aeolian Res.* 43, 100573. doi:10.1016/j.aeolia.2020.100573

Limarino, C., Tripaldi, A., Marenssi, S., and Fauqué, L. (2006). Tectonic, sealevel, and climatic controls on late Paleozoic sedimentation in the Western basins of Argentina. *J. S. Am. Earth Sci.* 33 (3–4), 205–226. doi:10.1016/j.jsames.2006.09.009

Lindzen, R. S., and Hou, A. V. (1988). Hadley Circulations for Zonally Averaged Heating Centered off the Equator. *J. Atmos. Sci.* 45 (17), 2416–2427. doi:10.1175/1520-0469(1988)045<2416:hcfzah>2.0.co;2

Lirer, L., Vinci, A., Alberico, I., Gifuni, T., Bellucci, F., Petrosino, P., et al. (2001). Occurrence of inter-eruption debris flow and hyperconcentrated flood-flow deposits on Vesuvio volcano, Italy. *Sediment. Geol.* 139 (2), 151–167. doi:10.1016/s0037-0738(00)00162-7

Liu, W., Carling, P. A., Hu, K., Wang, H., Zhou, Z., Zhou, L., et al. (2019). Outburst floods in China: A review. *Earth-Sci. Rev.* 197, 102895. doi:10.1016/j.earscirev.2019.102895

Liu, X., Lu, C., Li, X., Madsen, D., Wang, Y., Liu, Y., et al. (2020). Climate Conditions on the Tibetan Plateau During the Last Glacial Maximum and Implications for the Survival of Paleolithic Foragers. *Front. Earth Sci.* 8, 51. doi:10.3389/feart.2020.606051

López-Gamundí, O. R., Espejo, I. S., Conaghan, P. J., Powell, C. M., and Veevers, J. J. (1994). "Southern South America," in *Permian-triassic Pangea basins and foldbelts along the panthalassan margin of gondwanaland*. Editors J. Veevers and C. Powell (Geological Society of America Memoir), 184, 281–329.

López-Gamundí, O. R., Limarino, C. O., Isbell, J. L., Pauls, K., Césari, S. N., and Alonso Muruaga, P. (2021). The late Paleozoic Ice Age along the southwestern margin of Gondwana: Facies models, age constraints, correlation and sequence stratigraphic framework. *J. S. Am. Earth Sci.* 107, 103056. doi:10.1016/j.jsames.2020.103056

Mack, G. H. (1977). *Depositional environments of the Cutler–Cedar Mesa facies transition (Permian) near Moab*, 14. Utah: The Mountain Geologist, 53–68.

Mack, G. H., and Dinterman, P. A. (2002). Depositional environments and paleogeography of the Lower Permian (leonardian) Yeso and correlative formations in New Mexico. *Mt. Geol.* 39, 75–88.

Mack, G. H., and Rasmussen, K. A. (1984). Alluvial-fan sedimentation of the Cutler Formation (Permo-Pennsylvanian) near Gateway, Colorado: Geological Society of America. *Bulletin* 95, 109–116. doi:10.1130/0016-7606(1984)95<109:asotcf>2.0.co;2

Mackay, J. (1974). Ice-wedge cracks, Garry Island, Northwest Territories. *Can. J. Earth Sci.* 11, 1366–1383. doi:10.1139/e74-133

Mahaney, W. C., and Kalm, V. (1995). Scanning electron microscopy of Pleistocene tills in Estonia. *Boreas* 24, 13–29. doi:10.1111/j.1502-3885.1995.tb00624.x

Mahaney, W. C., and Kalm, V. (1996). *Field guide for the international conference on Quaternary glaciation and paleoclimate in the Andes Mountains*. Toronto: Quaternary Surveys.

Mahaney, W. C. (1995). Pleistocene and Holocene glacier thicknesses, transport histories and dynamics inferred from SEM microtextures on quartz particles. *Boreas* 24 (4), 293–304. doi:10.1111/j.1502-3885.1995.tb00781.x

Mahaney, W. C. (2002). *Atlas of sand grain surface textures and applications*. Oxford, U.K.: Oxford University Press, 237.

Mahaney, W. C., Vortsich, W., and Julig, P. J. (1988). Relative differences between glacially crushed quartz transported by mountain and continental ice, some examples from North America and East Africa. *Am. J. Sci.* 288, 810–826. doi:10.2475/ajs.288.8.810

Mahaney, W. C., Claridge, G., and Campbell, I. (1996). Microtextures on quartz grains in tills from Antarctica. *Palaeogeogr. Palaeoclimatol. Palaeoecol.* 121 (1-2), 89–103. doi:10.1016/0031-0182(95)00069-0

Maher, B. A. (2016). Palaeoclimatic records of the loess/palaeosol sequences of the Chinese Loess Plateau. *Quat. Sci. Rev.* 154 (C), 23–84. doi:10.1016/j.quascirev.2016.08.004

Maizels, J. (1989). Sedimentology, paleoflow dynamics and flood history of jokulhlaup deposits; paleohydrology of Holocene sediment sequences in

southern Iceland sandur deposits. *J. Sediment. Res.* 59 (2), 204–223. doi:10.1306/212F8F4E-2B24-11D7-8648000102C1865D

Maizels, J. (1993). Lithofacies variations within sandur deposits: the role of runoff regime, flow dynamics and sediment supply characteristics. *Sediment. Geol.* 85, 299–325. doi:10.1016/0037-0738(93)90090-r

Maizels, J. (1997). Jökulhlaup deposits in proglacial areas. *Quat. Sci. Rev.* 16, 793–819. doi:10.1016/s0277-3791(97)00023-1

Mallory, W. W. (1958). "Pennsylvanian coarse arkosic redbeds and associated mountains in Colorado," in *Symposium on pennsylvanian rocks of Colorado and adjacent areas: Rocky mountain association of geologists*. Editor B. Curtis, 17–20.

Maloof, A. C., Kellogg, J. B., and Anders, A. M. (2002). Neoproterozoic sand wedges: crack formation in frozen soils under diurnal forcing during a snowball Earth. *Earth Planet. Sci. Lett.* 204, 1–15. doi:10.1016/s0012-821x(02)00960-3

Mao, X., Liu, X., and Zhou, S. (2021). Permo-Triassic aeolian red clay of southwestern England and its palaeoenvironmental implications. *Aeolian Res.* 52, 100726. doi:10.1016/j.aeolia.2021.100726

Mark, W. D. (1932). Fossil Impressions of Ice Crystals in Lake Bonneville Beds. *J. Geol.* 40 (2), 171–176. doi:10.1086/623932

Marren, P. M. (2002). "Criteria for distinguishing high magnitude flood events in the proglacial fluvial sedimentary record,". *The extremes of the extremes: Extraordinary floods: International association of hydrological Sciences*. Editors A. Snorrason, H. P. Finnsdóttir, and M. E. Moss, 271, 237–241.

Marren, P. M. (2005). Magnitude and frequency in proglacial rivers: a geomorphological and sedimentological perspective. *Earth-Science Rev.* 70 (3-4), 203–251. doi:10.1016/j.earscirev.2004.12.002

Martgnier, L., Nussbaumer, M., Adatte, T., Gobat, J.-M., and Verrecchia, E. P. (2015). Assessment of a locally sourced loess system in Europe: The Swiss Jura Mountains. *Aeolian Res.* 18, 11–21. doi:10.1016/j.aeolia.2015.05.003

Matsuno, T. (1966). Quasi-geostrophic motions in the equatorial area. *J. Meteorol. Soc.* 44, 25–43. doi:10.2151/jmsj1965.44.1_25

Menéndez, I., Dıaz-Hernández, J. L., Mangasa, J., Alonsoa, I., and Sánchez-Soto, P. J. (2007). Airborne dust accumulation and soil development in the North-East sector of Gran Canaria (Canary Islands, Spain). *J. Arid Environ.* 71, 57–81. doi:10.1016/j.jaridenv.2007.03.011

Mitchell, S. G., and Montgomery, D. R. (2006). Influence of a glacial buzzsaw on the height and morphology of the Cascade Range in central Washington State, USA. *Quat. Res.* 65, 96–107. doi:10.1016/j.yqres.2005.08.018

Molén, M. O. (2014). A simple method to classify diamicts by scanning electron microscope from surface microtextures. *Sedimentology* 61 (7), 2020–2041. doi:10.1111/sed.12127

Moore, K. D., Soreghan, G. S., and Sweet, D. E. (2008). Stratigraphic and structural relations in the proximal Cutler Formation of the Paradox basin: Implications for timing of movement on the Uncompahgre fault. *Mt. Geol.* 45, 49–68.

Mote, P., and Kaser, G. (2007). The shrinking glaciers of Kilimanjaro: Can global warming be blamed? *Am. Sci.* 95 (4), 318. doi:10.1511/2007.66.318

Moxness, L. D., Isbell, J. L., Pauls, K. N., Limarino, C. O., and Schencman, J. (2018). Sedimentology of the mid-Carboniferous fill of the Olta paleovalley, eastern Paganzo Basin, Argentina: Implications for glaciation and controls on diachronous deglaciation in Western Gondwana during the late Paleozoic Ice Age. *J. S. Am. Earth Sci.* 84, 127–148. doi:10.1016/j.jsames.2018.03.015

Muhs, D. R., Bettis, E. A., III, and Skipp, G. L. (2018). Geochemistry and mineralogy of late Quaternary loess in the upper Mississippi River valley, USA: Provenance and correlation with Laurentide Ice Sheet history. *Quat. Sci. Rev.* 187, 235–269. doi:10.1016/j.quascirev.2018.03.024

Muhs, D. R., and Bettis, E. A.II (2003). "Quaternary loess-paleosol sequences as examples of climate-driven sedimentary extremes,". *Extreme depositional environments: Mega end members in geologic time: Boulder, Colorado*. Editors M. A. Chan and A. W. Archer (Boulder, CO: Geological Society of America Inc.), 370, 53–74. doi:10.1130/0-8137-2370-1.53

Muhs, D. R., Roskin, J., Tsoar, H., Skipp, G., Budahn, J. R., and Sneh, A. (2013). Origin of the Sinai-Negev erg, Egypt and Israel: Mineralogical and geochemical evidence for the importance of the Nile and sea level history. *Quat. Sci. Rev.* 69, 28–48. doi:10.1016/j.quascirev.2013.02.022

Murphy, K. (1987). *Eolian origin of upper Paleozoic red siltstones at Mexican Hat and Dark Canyon, southeastern Utah*. M.S. thesis. Lincoln, Nebraska: Lincoln, University of Nebraska, 128.

Myhre, G., Myhre, C., and Forster, P. (2017). Halfway to doubling of CO2 radiative forcing. *Nat. Geosci.* 10, 710–711. doi:10.1038/ngeo3036

Nartiss, M., and Kalinska-Nartisa, E. (2017). An aeolian or a glaciolacustrine record? A case study from Mielupite, Middle Guaja Lowland, northeast Latvia. *Geologos* 22, 15–28. doi:10.1515/logos-2017-0002

Neal, J. T. (1978). "Mudcracks (contractional polygons)," in *Encyclopedia of Sedimentology. Dowden, hutchinson and ross*. Editors R. W. Fairbridge and J. Bourgeois (Pennsylvania: Stroudsberg), 486–488.

Nemec, W., and Steel, R. J. (1984). "Alluvial and coastal conglomerates: their significant features and some comments on gravelly mass-flow deposits,". *Sedimentology of gravels and conglomerates*. Editors E. H. Koster and R. J. Steel, 10, 1–31. Can. Soc. Petrol. Geol., Mem.

Nesbitt, M. W., and Young, G. M. (1982). Early Proterozoic climates and plate motions inferred from major element chemistry of lutites. *Nature* 299, 715–717. doi:10.1038/299715a0

Neupane, R., Chen, H., and Cao, C. (2019). Review of moraine dam failure mechanism. *Geomatics, Nat. Hazards Risk* 10 (1), 1948–1966. doi:10.1080/19475705.2019.1652210

Nutz, A., Ghienne, J., and Storch, P. (2013). Circular, cryogenic structures from the hirnantian deglaciation sequence (Anti-Atlas, Morocco). *J. Sediment. Res.* 83, 115–131. doi:10.2110/JSR.2013.11

O'Connor, J. E., Beebee, R. A., and Burr, D. (2009). "Floods from natural rock-material dams," in *Megaflooding on earth and mars*. Editors D. Burr, P. Carling, and V. Baker (Cambridge: Cambridge University Press), 128–171. doi:10.1017/cbo9780511635632.008

Oordt, A. J., Soreghan, G. S., Stemmerik, L., and Hinnov, L. A. (2020). A record of dust deposition in northern, mid-latitude Pangaea during peak icehouse conditions of the late Paleozoic ice age. *J. Sediment. Res.* 90 (4), 337–363. doi:10.2110/jsr.2020.15

Patterson, A., Behm, M., Chwatal, W., Flores-Orozco, A., Wang, Y., and Soreghan, G. S. (2021). Seismic reflection and electrical resistivity imaging support pre-Quaternary glaciation in the Rocky Mountains (Unaweep Canyon, Colorado). *Geophys. Res. Lett.* 48, 18. doi:10.1029/2021GL094706

Pfeifer, L. S., Soreghan, G. S., Pochat, S., Van Den Driessche, J., and Thomson, S. N. (2016). Permian exhumation of the Montagne Noire core complex recorded in the Graissessac-Lodève Basin. *France. Basin Res.* 30 (Suppl 1), 1–14. doi:10.1111/bre.12197

Pfeifer, L. S., Soreghan, G. S., Pochat, S., and Van Den Driessche, J. (2020). Loess in eastern equatorial Pangea archives a dusty atmosphere and possible upland glaciation. *GSA Bull.* 133, 379–392. doi:10.1130/B35590.1

Pfeifer, L. S., Birkett, B. A., Van den Driessche, J., Pochat, S., and Soreghan, G. S. (2021). Ice-crystal traces imply ephemeral freezing in early Permian equatorial Pangea. *Geology* 49 (11), 1397–1401. doi:10.1130/G49011.1

Pierson, T. C., and Costa, J. E. (1987). A rheologic classification of subaerial sediment-water flows. *Geol. Soc. Am. Rev. Eng. Geol.* 7, 1–11. doi:10.1130/reg7-p1

Pierson, T. C. (2005). "Hyperconcentrated flow—transitional process between water flow and debris flow," in *Debris-flow hazards and related phenomena* (Berlin, Heidelberg: Springer), 159–202.

Pierson, T. C., and Scott, K. M. (1985). Downstream dilution of a lahar: Transition from debris flow to hypercocnetrated streamflow. *Water Resour. Res.* 21, 1511–1524. doi:10.1029/wr021i010p01511

Pippin, M. R. (2016). *Progressive downstream overprinting of glacially induced quartz microtextures during fluvial saltation, Salmon river, British Columbia, and Alaska*. MS Thesis. Texas, USA: Texas Tech University.

Priddy, C. L., and Clarke, S. M. (2020). The sedimentology of an ephemeral fluvial–aeolian succession. *Sedimentology* 67 (5), 2392–2425. doi:10.1111/sed.12706

Reahl, J. N., Cantine, M. D., Wilcots, J., Mackey, T. J., and Bergmann, K. D. (2021). Meta-analysis of Cryogenian through modern quartz microtextures reveals sediment transport histories. *J. Sediment. Res.* 91 (9), 929–944. doi:10.2110/jsr.2020.151

Reid, M. E., Coe, J. A., and Brien, D. L. (2016). Forecasting inundation from debris flows that grow volumetrically during travel, with application to the Oregon Coast Range, USA. *Geomorphology* 273, 396–411. doi:10.1016/j.geomorph.2016.07.039

Reineck, H. E. (1955). Marken, Spuren und Fährten in den Waderner Schichten (ro) bei Martinstein/Nahe. *Neues Jb. Geol. Palaont. Abh.* 101, 75–90.

Reiners, P. W., and Brandon, M. T. (2006). Using thermochronology to understand orogenic erosion. *Annu. Rev. Earth Planet. Sci.* 34, 419–466. doi:10.1146/annurev.earth.34.031405.125202

Retallack, G. J., Gose, B. N., and Osterhout, J. T. (2015). Periglacial paleosols and Cryogenian paleoclimate near Adelaide, South Australia. *Precambrian Res.* 263, 1–18. doi:10.1016/j.precamres.2015.03.002

Retallack, G. J. (2011). Neoproterozoic loess and limits to snowball Earth. *J. Geol. Soc. Lond.* 168, 289–307. doi:10.1144/0016-76492010-051

Rushmer, E. L., Russell, A. J., Tweed, F. S., Knudsen, O. S. K. A. R., and Marren, P. M. (2002). The role of hydrograph shape in controlling glacier outburst flood (joekulhlaup) sedimentation. *Int. Assoc. Hydrological Sci.* 276, 305–313.

Russell, A. J., and Marren, P. M. (1999). "Proglacial fluvial sedimentary sequences in Greenland and Iceland: A case study from active proglacial environments subject to jökulhlaups,". *The description and analysis of quaternary stratigraphic field sections*. Editors A. P. Jones, J. K. Hart, and M. E. Tucker (London: Quaternary Research Association Technical Guide), 7, 171–208.

Russell, A. J., Fay, H., Marren, P. M., Tweed, F. S., and Knudsen, Ó. (2005). Icelandic jökulhlaup impacts. *Icel. Mod. Process. past Environ.* 5, 153–203. doi:10.1016/s1571-0866(05)80009-0

Russell, J., Eggermont, H., Taylor, R., and Vershuren, D. (2009). Paleolimnological records of recent glacier recession in the Rwenzori Mountains, Uganda-D.R. Congo. *J. Paleolimnol.* 41, 253–271. doi:10.1007/s10933-008-9224-4

Santi, P. M., deWolfe, V. G., Higgins, J. D., Cannon, S. H., and Gartner, J. E. (2008). Sources of debris flow material in burned areas. *Geomorphology* 96, 310–321. doi:10.1016/j.geomorph.2007.02.022

Sardar Abadi, M., Owens, J. D., Liu, X., Them, T. R., II, Cui, X., Heavens, N. G., et al. (2020). Atmospheric dust stimulated marine primary productivity during Earth's penultimate icehouse. *Geol.* 48 (3), 247–251. doi:10.1130/G46977.1

Scott, K. M. (1988). "Origin, behavior, and sedimentology of prehistoric catastrophic lahars at Mount St. Helens, Washington,". Editor H. E. Clifton, 229, 23–36. doi:10.1130/spe229-p23*Sedimentologic Consequences Colvulsive Geol. Events Geol. Soc. Am. Special Pap.*

Scott, K. M., Vallance, J. W., and Pringle, P. T. (1995). *Sedimentology, behavior, and hazards of debris flows at Mount Rainer*. Washington: U.S. Geological Survey Professional Paper 1547, 56.

Shulmeister, J. (1989). Flood deposits in the Tweed Esker (southern Ontario, Canada). *Sediment. Geol.* 65, 153–163. doi:10.1016/0037-0738(89)90012-2

Shultz, A. W. (1984). Subaerial debris-flow deposition in the upper Paleozoic Cutler Formation, Western Colorado. *J. Sediment. Petrology* 54, 759–772. doi:10.1306/212F84EF-2B24-11D7-8648000102C1865D

Smalley, I. J., and Derbyshire, E. (1990). The definition of 'ice-sheet' and 'mountain' loess. *Area* 22, 300–301.

Smalley, I. J., and Krinsley, D. H. (1978). Loess deposits associated with deserts. *Catena* 5, 53–66. doi:10.1016/s0341-8162(78)80006-x

Smalley, I. J. (1966). The properties of glacial loess and the formation of loess deposits. *J. Sediment. Res.* 36 (3), 669–676. doi:10.1306/74D7153C-2B21-11D7-8648000102C1865D

Smalley, I. J. (1995). Making the material: The formation of silt-sized primary mineral particles for loess deposits. *Quat. Sci. Rev.* 14, 645–651. doi:10.1016/0277-3791(95)00046-1

Smalley, I. J., Jefferson, I. F., Dijkstra, T. A., and Derbyshire, E. (2001). Some major events in the development of the scientific study of loess. *Earth Sci. Rev.* 54, 5–18. doi:10.1016/s0012-8252(01)00038-1

Smalley, I. J., O'Hara-Dhand, K., Wint, J., Machalett, B., Jary, Z., and Jefferson, I. (2009). Rivers and loess: The significance of long river transportation in the complex event-sequence approach to loess deposit formation. *Quat. Int.* 198 (1–2), 7–18. doi:10.1016/j.quaint.2008.06.009

Smith, C., Soreghan, G. S., and Ohta, T. (2018). Scanning electron microscope (SEM) microtextural analysis as a paleoclimate tool for fluvial deposits: A modern test. *GSA Bull.* 130 (7-8), 1256–1272. doi:10.1130/b31692.1

Smith, G. A. (1986). Coarse-grained nonmarine volcaniclastic sediment: Terminology and depositional processes. *Geol. Soc. Am. Bull.* 97, 1–10. doi:10.1130/0016-7606(1986)97<1:cnvsta>2.0.co;2

Smith, G. A., and Lowe, D. R. (1991). "Lahars: volcano-hydrologic events and deposition in the debris flow—Hyperconcentrated flow continuum," in *Sedimentation in volcanic settings*. Editors R. V. Fisher and G. A. Smith (Tulsa, Oklahoma: SEPM Special Publication), 45, 59–70. doi:10.2110/pec.91.45.0059

Sohn, Y. K. (1997). On traction-carpet sedimentation. *J. Sediment. Res.* 67, 502–509. doi:10.1306/D42685AE-2B26-11D7-8648000102C1865D

Sohn, Y. K., Rhee, C. W., and Kim, B. C. (1999). Debris flow and hyperconcentrated flood-flow deposits in an alluvial fan, northwestern part of the Cretaceous Yongdong Basin, Central Korea. *J. Geol.* 107 (1), 111–132. doi:10.1086/314334

Soreghan, G. S., Elmore, R. D., and Lewchuk, M. T. (2002). Sedimentologic-magnetic record of Western Pangean climate in upper Paleozoic loessite (lower Cutler Beds, Utah). *Bull. Geol. Soc. Am.* 114 (8), 1019–1035. doi:10.1130/0016-7606(2002)114<1019:SMROWP>2.0.CO;2

Soreghan, G. S., Sweet, D. E., Marra, K. R., Eble, C. F., Soreghan, M. J., Elmore, R. D., et al. (2007). An exhumed late Paleozoic canyon in the Rocky Mountains. *J. Geol.* 115 (4), 473–481. doi:10.1086/518075

Soreghan, G. S., Soreghan, M. J., Poulsen, C. J., Young, R. A., Eble, C. F., Sweet, D. E., et al. (2008a). Anomalous cold in the Pangaean tropics. *Geology* 36, 659–662. doi:10.1130/g24822a.1

Soreghan, G. S., Soreghan, M. J., and Hamilton, M. A. (2008b). Origin and significance of loess in late Paleozoic Western Pangea: a record of tropical cold. *Palaeogeogr. Palaeoclimatol. Palaeoecol.* 268, 234–259. doi:10.1016/j.palaeo.2008.03.050

Soreghan, G. S., Soreghan, M. J., Sweet, D. E., and Moore, K. D. (2009). Hot fan or cold outwash? Hypothesized proglacial deposition in the upper Paleozoic Cutler Formation, Western tropical Pangea. *J. Sediment. Res.* 79 (7), 495–522. doi:10.2110/jsr.2009.055

Soreghan, G. S., Sweet, D. E., and Heavens, N. G. (2014). Upland glaciation in tropical Pangaea: Geologic evidence and implications for late Paleozoic climate modeling. *J. Geol.* 122 (2), 137–163. doi:10.1086/675255

Soreghan, G. S., Sweet, D. E., Thomson, S. N., Kaplan, S. A., Marra, K. R., Balco, G., et al. (2015). Geology of Unaweep Canyon and its role in the drainage evolution of the northern Colorado Plateau. *Geosphere* 11 (2), 320–341. doi:10.1130/GES01112.1

Soreghan, M. J., and Francus, P. (2004). "Processing backscattered electron digital images of thin section," in *Image analysis, sediments and paleoenvironments*. Editor P. Francus (Berlin: Springer), 203–225.

Soreghan, M. J., Heavens, N. G., Soreghan, G. S., Link, P. K., and Hamilton, M. A. (2014). Abrupt and high-magnitude changes in atmospheric circulation recorded in the Permian Maroon Formation, tropical Pangaea. *Geol. Soc. Amer. Bull.* 126 (3-4), 569–584. doi:10.1130/B30840.1

Spotila, J. A., Buscher, J. T., Meigs, A. J., and Reiners, P. W. (2004). Long-term glacial erosion of active mountain belts: example from the Chugach-St. Elias Range, Alaska. *Geology* 32, 501–504. doi:10.1130/g20343.1

Stuut, J.-B., Smalley, I., and O'Hara-Dhand, K. (2009). Aeolian dust in Europe: African sources and European deposits. *Quat. Int.* 198, 234–245. doi:10.1016/j.quaint.2008.10.007

Sur, S., Soreghan, G. S., Soreghan, M. J., Yang, W., and Saller, A. H. (2010). A record of glacial aridity and Milankovitch-scale fluctuations in atmospheric dust from the Pennsylvanian tropics. *J. Sediment. Res.* 80, 1046–1067. doi:10.2110/jsr.2010.091

Svendsen, J., Stollhofen, H., Krapf, C. B., and Stanistreet, I. G. (2003). Mass and hyperconcentrated flow deposits record dune damming and catastrophic breakthrough of ephemeral rivers, Skeleton Coast Erg, Namibia. *Sediment. Geol.* 160 (1-3), 7–31. doi:10.1016/s0037-0738(02)00334-2

Sweet, A. C., Soreghan, G. S., Sweet, D. E., Soreghan, M. J., and Madden, A. S. (2013). Permian dust in Oklahoma: Source and origin for Middle Permian (Flowerpot-Blaine) redbeds in Western tropical Pangaea. *Sediment. Geol.* 284–285, 181–196. doi:10.1016/j.sedgeo.2012.12.006

Sweet, D. E., and Brannan, D. K. (2016). Proportion of glacially to fluvially induced quartz grain microtextures along the Chitina River, SE Alaska, USA. *J. Sediment. Res.* 86 (7), 749–761. doi:10.2110/jsr.2016.49

Sweet, D. E. (2017). Fine-grained debris flows in coarse-grained alluvial systems: Paleoenvironmental implications for the late Paleozoic Fountain and Cutler formations, Colorado, U.S.A. *J. Sediment. Res.* 87, 763–779. doi:10.2110/jsr.2017.45

Sweet, D. E., and Soreghan, G. S. (2008). Polygonal cracking in coarse clastics records cold temperatures in the equatorial Fountain Formation (Pennsylvanian-Permian, Colorado). *Palaeogeogr. Palaeoclimatol. Palaeoecol.* 268, 193–204. doi:10.1016/j.palaeo.2008.03.046

Sweet, D. E., and Soreghan, G. S. (2010a). Application of quartz sand microtextural analysis to infer cold-climate weathering for the equatorial Fountain Formation (Pennsylvanian-Permian, Colorado, USA). *J. Sediment. Res.* 80, 666–677. doi:10.2110/jsr.2010.061

Sweet, D. E., and Soreghan, G. S. (2010b). Late Paleozoic tectonics and paleogeography of the Ancestral Front Range: structural, stratigraphic and sedimentological evidence from the Fountain Formation (Manitou Springs, Colorado). *Geol. Soc. Am. Bull.* 122, 575–594. doi:10.1130/b26554.1

Swet, N., Elperin, T., Kok, J. F., Martin, R. L., Yizhaq, H., and Katra, I. (2019). Can active sands generate dust particles by wind-induced processes? *Earth Planet. Sci. Lett.* 506, 371–380. doi:10.1016/j.epsl.2018.11.013

Todd, S. P. (1989). Stream-driven, high-density gravelly traction carpets: possible deposits in the Traberg Conglomerate Formation, SW Ireland and some theoretical considerations of their origin. *Sedimentology* 36, 513–530. doi:10.1111/j.1365-3091.1989.tb02083.x

Tooth, S., Hancox, P. J., Brandt, D., McCarthy, T. S., Jacobs, Z., and Woodborne, S. (2013). Controls on the Genesis, sedimentary architecture, and preservation potential of

dryland alluvial successions in stable continental interiors: insights from the incising Modder River, South Africa. *J. Sediment. Res.* 83 (7), 541–561. doi:10.2110/jsr.2013.46

Tramp, K. L., Soreghan, G. S., and Elmore, R. D. (2004). Paleoclimatic inferences from paleopedology and magnetism of the Permian Maroon Formation loessite (Colorado, USA). *Geol. Soc. Am. Bull.* 116, 671–686. doi:10.1130/b25354.1

Tsoar, H., and Pye, K. (1987). Dust transport and the question of desert loess formation. *Sedimentology* 34, 139–153. doi:10.1111/j.1365-3091.1987.tb00566.x

Tutkovskii, P. A. (1899). The question of the method of loess formation. *Zemlevedenie* 1–2, 213–311. in Russian: see Loess Letter Supplement 16, 1986.

Udden, J. A. (1918). Fossil Ice Crystals. *Univ. Tex. Bull.* 1821, 3–39.

Valdez-Buso, V., Milana, J. P., di Pasquo, M., and Aburto, J. E. (2020). The glacial paleovalley of Vichigasta: Paleogeomorphological and sedimentological evidence for a large continental ice-sheet for the mid-Carboniferous over central Argentina. *J. S. Am. Earth Sci.* 106, 103066. doi:10.1016/j.jsames.2020.103066

Vallis, G. K., and Penn, J. (2020). Convective organization and eastward propagating equatorial disturbances in a simple excitable system. *Q. J. R. Meteorol. Soc.* 146, 2297–2314. doi:10.1002/qj.3792

Vandenberghe, J. (2013). Grain size of fine-grained windblown sediment: A powerful proxy for process identification. *Earth Sci. Rev.* 121 (C), 18–30. doi:10.1016/j.earscirev.2013.03.001

Voigt, S., Oliver, K., Small, B. J., Geoskop, U., and Lichtenberg, B. (2021). Potential ice crystal marks from Pennsylvanian-Permian equatorial red-beds of northwest Colorado, USA. *PALAIOS* 36 (12), 377–392. doi:10.2110/palo.2021.024

Waitt, R. B., Jr., Pierson, T. C., MacLeod, N. S., Janda, R. J., Voight, B., and Holcomb, R. T. (1983). Eruption-triggered avalanche, flood, and lahar at Mount St. Helens—effects of winter snowpack. *Science* 221, 1394–1396. doi:10.1126/science.221.4618.1394

Wan, Z., and Wang, Z. (1994). "Hyperconcentrated flow," in *International association of hydraulic research monograph series* (Rotterdam: A. A. Balkema), 290.

Washington, R., Todd, M. C., Lizcano, G., Tegen, I., Flamant, C., Koren, I., et al. (2006). Links between topography, wind, deflation, lakes and dust: The case of the Bodele Depression. *Chad. Geophys. Res. Lett.* 33, L09401. doi:10.1029/2006GL025827

Wegener, A. (1929). *The origin of continents and oceans (English translation by J. Biram, 1996, of Die Entstehung der Kontinente and Ozeane, revised*. 4th edition, 246. Braunschweig, Germany Friedr: Dover Publications, Inc.. Vieweg & Sohn: New York.

Weinberger, R. (2001). Evolution of polygonal patterns in stratified mud during desiccation: The role of flaw distribution and layer boundaries. *Geol. Soc. Am. Bull.* 113, 20–31. doi:10.1130/0016-7606(2001)113<0020:eoppis>2.0.co;2

Werner, W. G. (1974). Petrology of the Cutler Formation (Pennsylvanian–Permian) near Gateway, Colorado, and Fisher Towers, Utah. *J. Sediment. Petrology* 44, 292–298. doi:10.1306/74D72A18-2B21-11D7-8648000102C1865D

Whalley, W. B., Smith, B. J., McAlister, J. J., and Edwards, A. J. (1987). "Aeolian abrasion of quartz particles and the production of silt-size fragments: Preliminary results,". *Desert sediments: Ancient and modern*. Editors L. E. Frostick and I. Reid (London: Geological Society), 35, 129–138. doi:10.1144/gsl.sp.1987.035.01.09

Whipple, K. X. (2009). The influence of climate on the tectonic evolution of mountain belts. *Nat. Geosci.* 2, 97–104. doi:10.1038/ngeo413

Wilkins, A. D., Hurst, A., Wilson, M. J., and Archer, S. (2018). Paleo-environment in an ancient, low-latitude, arid lacustrine basin with loessite: The Smith Bank Formation (Early Triassic) in the Central North Sea, UK Continental Shelf. *Sedimentology* 65, 335–359. doi:10.1111/sed.12382

Wilson, M. J., Hurst, A., Wilkins, A. D., Wilson, L., and Bowen, L. (2020). Mineralogical evidence for multiple dust sources in an early Triassic loessite. *Sedimentology* 67, 239–260. doi:10.1111/sed.12641

Winspear, N. R., and Pye, K. (1995). Textural, geochemical, and mineralogical evidence for the origin of Peoria Loess in central and southern Nebraska, USA. *Earth Surf. Process.* 20, 735–745. doi:10.1002/esp.3290200805

Witus, A. E., Branecky, C. M., Anderson, J. B., Szczuciński, W., Schroeder, D. M., Blankenship, D. D., et al. (2014). Meltwater intensive glacial retreat in polar environments and investigation of associated sediments: example from Pine Island Bay, West Antarctica. *Quat. Sci. Rev.* 85, 99–118. doi:10.1016/j.quascirev.2013.11.021

Wong, T. E., Cui, Y., and Royer, D. L. (2021). A tighter constraint on Earth-system sensitivity from long-term temperature and carbon-cycle observations. *Nat. Commun.* 12, 3173. doi:10.1038/s41467-021-23543-9

Wright, J. (2001). Making loess-sized quartz silt: Data from laboratory simulations and implications for sediment transport pathways and the formation of "desert" loess deposits associated with the Sahara. *Quat. Int.* 76 (77), 7–19. doi:10.1016/s1040-6182(00)00085-9

Wright, J., Smith, B., and Whalley, B. (1998). Mechanisms of loess-sized quartz silt production and their relative effectiveness: Laboratory simulations. *Geomorphology* 23, 15–34. doi:10.1016/s0169-555x(97)00084-6

Wu, Z., Sarachik, E. S., and Battisti, D. S. (2001). Thermally Driven Tropical Circulations under Rayleigh Friction and Newtonian Cooling: Analytic Solutions. *J. Atmos. Sci.* 58 (7), 724–741. doi:10.1175/1520-0469(2001)058<0724:tdtcur>2.0.co;2

Xiangang, J., Peng, C., Huayong, C., and Yayong, G. (2017). Formation conditions of outburst debris flow triggered by overtopped natural dam failure. *Landslides* 14, 821–831. doi:10.1007/s10346-016-0751-1

Xie, X., Duan, A., Shi, Z., Li, X., Sun, H., Liu, X., et al. (2020). Modulation of springtime surface sensible heating over the Tibetan Plateau on the interannual variability of East Asian dust cycle. *Atmos. Chem. Phys.* 20, 11143–11159. doi:10.5194/acp-20-11143-2020

Ye, D. (1981). Some Characteristics of the Summer Circulation Over the Qinghai-Xizang (Tibet) Plateau and Its Neighborhood. *Bull. Am. Meteorological Soc.* 62 (1), 14–19. doi:10.1175/1520-0477(1981)062<0014:scotsc>2.0.co;2

Zhisheng, A., Kutzbach, J., and Prell, W. (2001). Evolution of Asian monsoons and phased uplift of the Himalaya–Tibetan plateau since Late Miocene times. *Nature* 411, 62–66. doi:10.1038/35075035

Zielinski, T., and Van Loon, A. J. (2003). Pleistocene sandur deposits represent braidplains, not alluvial fans. *Boreas* 32, 590–611. doi:10.1080/03009480310004170

Zieliński, T., and Van Loon, A. J. (1998). Subaerial terminoglacial fans I: a semi-quantitative sedimentological analysis of the proximal environment. *Geol. Mijnb.* 77 (1), 1–15. doi:10.1023/A:1003535101480

Zieliński, T., and Van Loon, A. J. (1999). Subaerial terminoglacial fans II: a semi-quantitative sedimentological analysis of the middle and distal environments. *Geol. Minbouw* 78 (1), 73–85. doi:10.1023/A:1003862730530